



This is an accepted version of the following published document:

Nora Richter, James M. Russell, Linda Amaral-Zettler, Wylie DeGroff, Pedro M. Raposeiro, Vítor Gonçalves, Erik J. de Boer, Sergi Pla-Rabes, Armand Hernández, Mario Benavente, Catarina Ritter, Alberto Sáez, Roberto Bao, Ricardo M. Trigo, Ricardo Prego, Santiago Giralt, Long-term hydroclimate variability in the sub-tropical North Atlantic and anthropogenic impacts on lake ecosystems: A case study from Flores Island, the Azores, *Quaternary Science Reviews*, Volume 285, 2022, 107525, ISSN 0277-3791, <https://doi.org/10.1016/j.quascirev.2022.107525>.
(<https://www.sciencedirect.com/science/article/pii/S0277379122001561>)



© 2022. This manuscript version is made available under the CC-BY-NC-ND 4.0 license: <https://creativecommons.org/licenses/by-nc-nd/4.0>.



UNIVERSIDADE DA CORUÑA

**Long-term hydroclimate variability in the sub-tropical North Atlantic and
anthropogenic impacts on lake ecosystems: A case study from Flores Island, the
Azores**

Nora Richter^{a, b, 1*}, James M. Russell^a, Linda Amaral-Zettler^{a, b, c, d}, Wylie DeGroot^a, Pedro
M. Raposeiro^{e, f}, Vítor Gonçalves^{e, f}, Erik J. de Boer^j, Sergi Pla-Rabes^{g, h}, Armand
Hernándezⁱ, Mario Benavente^j, Catarina Ritter^e, Alberto Sáez^k, Roberto Bao^l, Ricardo
Trigo^l, Ricardo Prego^m, and Santiago Giral^l

^a*Department of Earth, Environmental and Planetary Sciences, Brown University,
Providence, RI 02912, USA*

^b*The Josephine Bay Paul Center for Comparative Molecular Biology and Evolution,
Marine Biological Laboratory, Woods Hole, MA, 02543, USA*

^c*Department of Marine Microbiology and Biogeochemistry, NIOZ Royal Netherlands Institute for Sea Research, AB
Den Burg, The Netherlands*

^d*Department of Freshwater and Marine Ecology, Institute for Biodiversity and Ecosystem Dynamics, University of
Amsterdam, Amsterdam, The Netherlands*

^e*Centro de Investigação em Biodiversidade e Recursos Genéticos, CIBIO, InBIO Laboratório Associado, Pólo dos
Açores, Portugal*

^f*Faculdade de Ciências e Tecnologia da Universidade dos Açores, Ponta Delgada, Açores, Portugal*

^g*CREAF & UAB, Cerdanyola del Vallès, Barcelona, Spain*

^h*Department of Geography, Environmental Management and Energy Studies, University of Johannesburg, Corner
Ditton and University Avenue, Auckland Park, Johannesburg, South Africa*

ⁱ*Universidade da Coruña, GRICA Group, Centro de Investigacións Científicas
Avanzadas (CICA), Rúa as Carballeiras, 15071, A Coruña, Spain*

^j*Geosciences Barcelona (GEO3BCN-CSIC), Spanish National Research Council, Barcelona, Spain*

^k*UB-Geomodels Research Institute. Department of Earth and Ocean Dynamics, Universitat de Barcelona,
Barcelona, Spain*

^l*Instituto Dom Luiz (IDL), Faculty of Sciences, University of Lisboa, Lisbon, Portugal*

^m*Marine Research Institute (IIM), Spanish National Research Council (CSIC), Vigo, Spain*

***Corresponding author: Nora Richter**

Email: nora.richter@nioz.nl

¹*Present address: NIOZ Royal Netherlands Institute for Sea Research, P.O. Box 59, 1790 AB Den Burg, The
Netherlands*

Highlights:

- High-resolution paleoclimate and paleoecological reconstruction from Flores Island
- Multi-proxy records distinguish human impacts from climate change
- Early human settlers lowered the resilience of lake ecosystems on remote islands

1 **Abstract**

2 Human land use and climate change threaten ecosystems and natural resources,
3 particularly on remote islands such as the Azores Archipelago in the North Atlantic. Since the
4 official Portuguese settlement of the archipelago in the 15th and 16th centuries humans have
5 extensively modified the Azorean landscape, with invasive plants dominating the present-day
6 vegetation and evidence of eutrophication in numerous lakes. To evaluate changes in terrestrial
7 and aquatic ecosystems in the Azores, we developed paleoecological and paleoclimate records
8 from Lake Funda on Flores Island that span the last millennium. Changes in precipitation
9 amount, as recorded by hydrogen isotopes from C₃₀ fatty acids (δD_{wax}), suggest that the climate
10 was relatively stable between c. 1000-1400 CE. Recent evidence of early human settlers on the
11 Azorean islands (c. 850-1300 CE) suggests that the introduction of livestock led to an increase in
12 primary productivity in Lake Funda and other lakes in the Azores. More depleted δD_{wax} values
13 between c. 1500-1620 CE suggest that wetter climate conditions existed during the establishment
14 of permanent settlements on Flores Island. Landscape changes between c. 1500-1600 CE
15 coincided with an increase in primary productivity and hypoxic conditions in the lake bottom
16 water, signifying the eutrophication of Lake Funda. Despite reforestation efforts in the Azores in
17 the early 20th century and shift towards drier conditions, eutrophication in Lake Funda persisted.
18 Reforestation efforts likely reduced nutrient leaching and soil erosion in the catchment area of
19 Lake Funda and other Azorean lakes, yet eutrophication continues to be widespread. This
20 highlights the lasting impacts of early human settlers on Lake Funda, and the need for more
21 active remediation efforts.

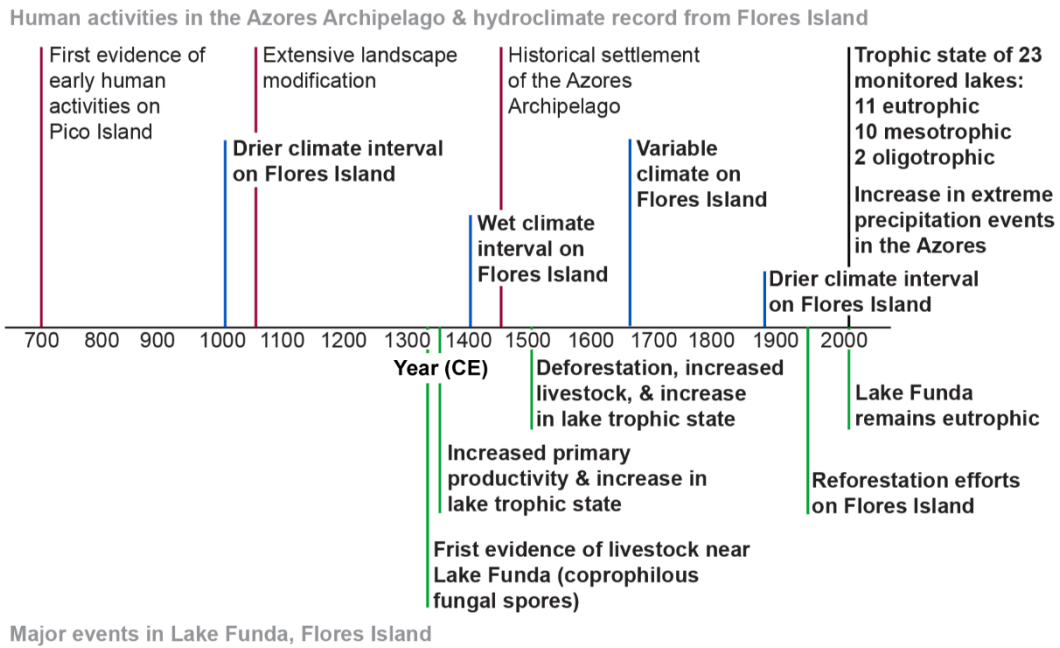
22

23

24

25 **Keywords:** Paleoecology; paleoclimate; eutrophication; North Atlantic; hydroclimate; land-use
26 change

27
28 **Graphical Abstract:**
29
30



31

32 **1. Introduction**

33 Rising sea levels, changing precipitation patterns, and warmer temperatures threaten
34 island ecosystems that are already under pressure from anthropogenic land use changes (Frias,
35 2000; Santos et al., 2004; Hoegh-Guldberg et al., 2018). Portuguese settlers shaped the landscape
36 of the Azores Archipelago by replacing dense native laurel forests with exotic plants and
37 agricultural fields, which led to increased soil erosion and left only a few places with native flora
38 and fauna (Dias et al., 2005; Connor et al., 2012; Rull et al., 2017; Raposeiro et al., 2021b).
39 Today the islands are at risk from landslides (Marques et al., 2008), storms and floods (Andrade
40 et al., 2008), and coastal erosion (Calado et al., 2011), and this risk is expected to increase under
41 projected climate change scenarios (Frias, 2000; Santos et al., 2004; Hoegh-Guldberg et al.,
42 2018; Gordo et al., 2019). Although the broad outlines of this history are generally accepted, a
43 more in-depth assessment of past land use changes and climate variability is needed to
44 understand the current state and vulnerability of terrestrial and aquatic ecosystems in the Azores
45 and how past changes in climate influenced human settlement of the islands.

46 The historically-accepted timing of the settlement of the Azores is close to the onset of
47 the Little Ice Age (LIA, c. 1450-1850 CE), although it is unclear whether this occurred during a
48 wetter or drier climate interval in the subtropical North Atlantic region (Björck et al., 2006;
49 Hernández et al., 2017). Historical records from the 15th century describe the slow establishment
50 and abandonment of early settlements in the central and westernmost islands of the Azores
51 Archipelago due to the isolated location of these islands, infertile land, and/or harsh climate
52 conditions (Smith, 2010). Paleorecords, however, suggest the Azores Archipelago was already
53 inhabited c. 700 years (between c. 700-850 CE) before the arrival of the Portuguese in the 15th
54 century (Raposeiro et al., 2021b). It is unclear whether these settlements persisted until the 15th

55 century, or if they were abandoned before the arrival of the Portuguese. A high-resolution
56 reconstruction of precipitation changes in the Azores and a complementary record of human land
57 use changes could provide insights on how climate change over the last millennium influenced
58 the settlement of the Azores Archipelago, in particular the settlement of Flores Island.

59 The ongoing eutrophication in Azorean lakes is attributed to human activities, including
60 indirect effects such as nutrient loading from the catchment area and direct effects such as fish
61 introductions (Skov et al., 2010; Antunes & Rodrigues, 2011; Cruz et al., 2015; Raposeiro et al.,
62 2017; Vázquez-Loureiro et al., 2019). However, these effects do not explain the high rates of
63 eutrophication observed in lakes isolated from direct human impacts (Antunes & Rodrigues,
64 2011). For instance, Lake Funda on Flores Island is considered to be less impacted by human
65 activities relative to the rest of the Azores Archipelago (Connor et al., 2012), but in the present-
66 day it is considered eutrophic based on high turbidity measurements, as well as nutrient
67 concentrations (i.e., phosphorous) and chlorophyll- α levels (Fig. S1; Cordeiro et al., 2020). It is
68 unclear whether this eutrophication is natural, reflects human modifications in the past, or both.
69 Rising temperatures, changing precipitation patterns, and continued human activities all pose
70 potential risks to these freshwater ecosystems, and threaten their value as a natural resource for
71 the archipelago (Antunes & Rodrigues, 2011).

72 To understand the role of humans and natural climate variability in shaping the present-
73 day landscape, we developed paleoecological and paleoclimate records for Lake Funda on Flores
74 Island. Fecal biomarkers and shifts in vegetation composition indicate when human activities
75 began in the catchment area. In addition, bulk organic and inorganic geochemical proxies, sterol
76 hydrogenation, and archaeal lipids trace changes in organic matter inputs to the lake, redox
77 conditions, and biogeochemical cycles, respectively. Finally, a high-resolution reconstruction

78 using leaf wax hydrogen isotopes records changes in precipitation amount over the last
79 millennium. We investigate the relationships among these variables to determine the interactive
80 effects of climate variations and human activities on Azorean environmental systems.

81

82 **2. Methods**

83 *2.1 Study site*

84 The climate in the Azores is strongly influenced by the Azores anticyclone, leading to
85 increased precipitation from September to March (monthly average precipitation 112 mm) when
86 the storm tracks cross the islands and drier conditions during the late spring and summer months
87 (monthly average precipitation 59 mm) (Santos et al., 2004; Hernández et al. 2016; Global
88 Historical Climatology Network (GHCN)). Maritime conditions result in mild temperatures with
89 mean annual temperatures of 18°C on Flores Island (GHCN).

90 Lake Funda occupies a maar with a 0.37 km² surface area, a steep bathymetric gradient,
91 and maximum depth of 35.3 m. The lake is located 351 m a.s.l. at 39°24'N 31°13'W (Figure 1).

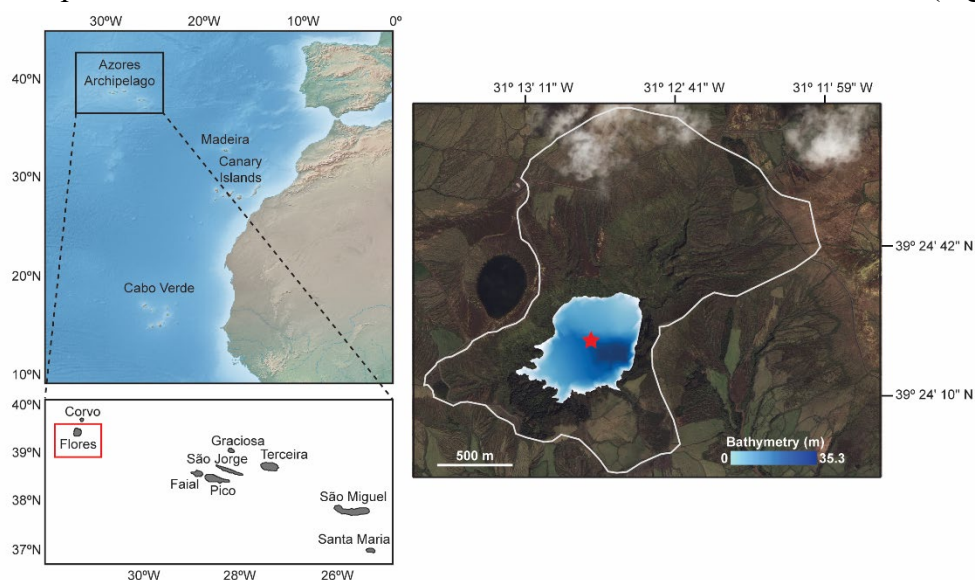


Figure 1. The islands that make up Macaronesia are shown with a close-up of the Azores Archipelago. Lake Funda is located on Flores Island. The bathymetry of Lake Funda is shown and the location of the core analyzed in this study is marked by a red star. The white line outlines the catchment area of Lake Funda. Raster data was obtained from Natural Earth and the maps were rendered in Matlab and ArcGIS.

92 It is located in the interior of Flores Island in the Azores Archipelago and is surrounded by a
93 relatively large (3.14 km²) and steep catchment area that is mostly forested with some agriculture
94 (Andrade et al., 2019). The lake is monomictic as the lake thermally stratifies from the summer
95 to fall (usually May/June to November) and the water column mixes from November/December
96 to May/June. The lake is considered eutrophic and is usually phosphorus limited (Figure S1).
97 Heightened primary productivity during the spring/summer can lead to rapid oxygen depletion in
98 the water column and hypoxic conditions in the bottom water that leads to internal phosphorus
99 loading (Figure S2).

100

101 *2.3 Sample preparation and analysis*

102 We used a UWITEC[®] piston corer installed on a UWITEC[®] platform to retrieve sediment
103 cores from Lake Funda in June 2017 at a water depth of 28.2 m. A total of 9.95 m of sediment
104 were recovered, sealed, and shipped to the Geosciences Barcelona (GEO3BCN-CSIC), where
105 they were kept in a dark room at +4 °C until they were prepared for analysis. In June 2018, we
106 collected soil samples to differentiate lipids derived from the catchment area from those
107 produced within the lake water column. Soil samples were shipped to the NIOZ Royal
108 Netherlands Institute for Sea Research and were stored at +4 °C in a dark room until the samples
109 were processed and analyzed for lipids.

110 Cores were split longitudinally and imaged using the high-resolution line scan camera
111 installed on the XRF AVAATECH Core Scanner at the Universitat de Barcelona (UB). Samples
112 were measured for total carbon (TC) and total nitrogen (TN) and the respective isotopic values
113 ($\delta^{13}\text{C}$ and $\delta^{15}\text{N}$) as described in Raposeiro et al. (2021b). Briefly, samples were analyzed using a
114 ThermoFinnigan Flash- EA1112 elemental analyzer (Thermo Fisher Scientific, Waltham, MA,

115 USA), connected on line to a ThermoFinnigan Deltaplus isotope ratio mass spectrometer
116 (IRMS), at the Servizos de Apoio á Investigación of the Universidade da Coruña (SAI-UDC).
117 Mineralogical analyses were performed with a Bruker D8-A25 diffractometer equipped with a
118 Cu tube ($\lambda=1.5405 \text{ \AA}$) and an ultrafast position sensitive detector (PSD) at the Geo3BCN-
119 CSIC. The carbonate content of these samples was below the detection limit of the X-ray
120 diffractometer, and therefore TC was considered to be equivalent to total organic carbon (TOC).
121 TOC/TN (or C/N) molar ratios were calculated for all measured samples. X-Ray Fluorescence
122 (XRF) was measured on the archived half of the core with the AVAATECH XRF II core scanner
123 at 2 mm intervals. Biogenic silica (BSi) content was determined every 4 cm following Bernárdez
124 et al. (2005) and Mortlock and Froelich (1989), using an Auto Analyzer Technicon AAII at the
125 Marine Research Institute (CSIC) in Vigo.

126 The cores were sampled for lipid analyses, which were processed and analyzed at Brown
127 University and NIOZ. Sediment and soil samples were freeze-dried and lipids were extracted
128 using a DionexTM accelerated solvent extraction (ASE 350) system with
129 dichloromethane:methanol (DCM:MeOH, 9:1 v/v) at 120°C and 1200 psi. The resulting
130 extracts were split, with one aliquot processed for glycerol dialkyl glycerol tetraethers (GDGTs)
131 and *n*-alkanes and the other prepared for fatty acid and sterol and stanol analyses.

132 The aliquot for GDGT samples was separated using aluminum oxide (Al_2O_3) columns to
133 obtain a non-polar (hexane (Hex):DCM, 9:1 v/v) fraction containing *n*-alkanes and a polar
134 (DCM:MeOH, 1:1 v/v) fraction for GDGTs. The resulting polar fraction was dried using N_2 gas,
135 and re-dissolved in Hex:Isopropanol (99:1, v/v) and filtered through a 0.4 μm PTFE prior to
136 analysis.

137 The acid/polar fraction was separated into neutral (DCM:Isopropanol, 2:1, v/v) and acid
138 (ethyl ether:acetic acid, 24:1, v/v) fractions using an aminopropylsilyl (NH₂) column. The acid
139 fraction was methylated at 60°C for 2 hrs with acidified anhydrous methanol of a known isotopic
140 composition, and the resulting fatty acid methyl ethers (FAMES) were purified via silica gel (40-
141 63 μm, 60 Å) flash chromatography. The neutral fraction was further separated by silica gel flash
142 chromatography into alkane (Hex), ketone (DCM), and polar (MeOH) fractions. The polar
143 fraction was saponified by dissolving the sample in a 1 M potassium hydroxide solution with
144 MeOH:H₂O (95:5, v/v) and heating it for 3 hrs at 65°C. To this 5% NaCl in H₂O and 50%
145 HCl in H₂O was added, and the lipid fraction was extracted using Hex (100%). The
146 saponified samples were cleaned on a short silica gel column and dried using N₂ gas for
147 derivatization. Pyridine (50 μL) and N,O-Bis(trimethylsilyl)trifluoroacetamide (BSTFA, 50
148 μL) were added to the dried sample, and the sample was capped under N₂ gas and heated for
149 2 hrs at 60°C. The derivatized samples were stored in pyridine until analysis, during which
150 they were dried and re-dissolved in toluene.

151 Samples for GDGTs were analyzed at NIOZ using an Atmospheric Pressure Chemical
152 Ionization/High Performance Liquid Chromatography-Mass Spectrometer (APCI/HPLC-MS)
153 following the method described in Hopmans et al. (2016). An additional 19 samples and
154 replicates were analyzed at Brown University using an APCI/HPLC-MS using the method
155 described in Hopmans et al. (2016). All GDGT results are reported as fractional abundances in
156 this study and concentrations are included for the available samples in the full dataset. The
157 analyses were run using selective ion monitoring to track *m/z* 1302, 1300, 1298, 1296, 1292,
158 1050, 1048, 1046, 1036, 1034, 1032, 1022, 1020, 1018, and 744. This study focuses on

159 isoprenoidal GDGTs (isoGDGTs), but we also quantified and report on branched GDGTs
160 (brGDGTs) in our dataset.

161 All *n*-alkanes and fatty acids were quantified with an Agilent 6890N gas chromatography
162 (GC) system and a flame ionization detector (FID) at Brown University. Samples were injected
163 using pulsed splitless mode (20.3 psi, 310°C) onto a Rtx-200 column (105 m x 205 µm x 0.25
164 µm). The oven program was started at 50°C, ramped up to 315°C at 10°C/min, and then held
165 isothermally for 30 min. All *n*-alkanes were quantified by using hexamethylbenzene as an
166 internal standard.

167 Compound specific isotope ratios (δD_{wax}) of C₃₀ FAMES were measured on an Agilent
168 6890 GC equipped with a ZB-1MS (30 m x 320 µm x 0.25 µm) coupled to a Thermo Delta V
169 Plus Isotope Ratio Mass Spectrometer (IRMS) at Brown University. The GC method was run
170 using a pulsed splitless injection mode (30 psi, 320°C), and the oven program was started at
171 40°C for 1 min, and then ramped up to 230°C at 30°C/min where it was held for 1 min. The
172 temperature was increased again to 310°C at 10°C/min and held isothermally for 10 min. The
173 pyrolysis reactor temperature for the IRMS was set at 1450°C. The reference gas ²H/¹H was
174 measured using certified C₂₉ and C₃₁ *n*-alkane standards. The H³⁺ factor was determined every
175 day, and the mean over the period that samples were measured was 2.41 ± 0.07. An internal
176 standard mixture containing C₁₆, C₁₈, C₂₂, C₂₄, C₂₈, and C₃₀ *n*-acids (see Table S1 for analytical
177 uncertainty) was analyzed between every 3 to 4 injections to monitor instrument performance
178 and drift, and a certified C₃₀ methyl ester standard of known composition was run to monitor
179 instrument accuracy (lab measured: -186.4 ± 3.9 ‰ for n = 71, actual: -189.4 ± 2 ‰ for n = 5;
180 Schimmelmann, 2018). Each sample was measured three times, and isotopic values were
181 accepted for a voltage response between 2.5 and 7 volts. Isotopic measurements were corrected

182 for the added methyl group, where $\delta D_{MeOH} = -123.7 \text{ ‰}$ (Tierney et al., 2011). Corrections were
183 made on a daily basis for offsets between measured and reported standard values. All δD_{wax}
184 values are reported relative to the Vienna Standard Mean Ocean Water (VSMOW) in per mil
185 (‰) notation.

186 Sterol and stanol samples were analyzed on an Agilent 7890B gas chromatography
187 (GC) system equipped with an Agilent 5977B quadrupole mass spectrometer (MS) at Brown.
188 Samples were injected using pulsed splitless mode (320°C, 1.3 psi) and run on a ZB-1MS (30 m
189 x 320 μm x 0.25 μm) column. The oven program was started at 40°C for 1 min, and then ramped
190 up to 255°C at 20°C/min and ramped to 315°C at 4°C/min and held isothermally for 10 min. The
191 MS ionization energy was set to 70 eV with a scan range of m/z 50-650. Samples were quantified
192 using select ion monitoring mode and concentrations were determined using 5 α -cholestan-3-one
193 as an internal standard (see Table S2).

194

195 2.2 Age model

196 We developed the age-depth model (Fig. S3) using ^{210}Pb and ^{137}Cs concentration profiles
197 and ^{14}C dates measured on plant macrofossils in the sediment core (Table S3) as described in
198 Raposeiro et al. (2021b). All radiocarbon dates were calibrated to calendar years (cal yr CE)
199 using the CALIB 7.1 software and the latest INTCAL20 curve (Reimer et al., 2020). In the lower
200 half of the sedimentary sequence (S4), six layers corresponding to gravelly alluvial sediments,
201 rich in terrestrial plant remains that were deposited as single, instantaneous episodic flood
202 events, were removed from the age model. The final age model was developed using the R
203 package clam version 2.3.9 (Blaauw, 2020). The confidence interval of the resulting age-depth
204 model fluctuates between 1 and 50 years throughout the record. In the age-depth model there is a

205 significant increase in the sedimentation rate at 221 cm of core depth which coincides with a
206 lithological change from massive-brown silty clays to centimeter-thick laminated green and
207 yellowish clays. This lithological change was interpreted as deepening in the lake water column
208 (Ritter et al., 2022).

209

210 *2.4 Data processing and breakpoint analysis*

211 Lipid and sediment fluxes were calculated using changes in dry bulk density and
212 sedimentation rates in the sediment core. Potential changes in preservation conditions were
213 assessed by normalizing lipid concentrations to total organic carbon. To determine when
214 significant changes occurred in the sediment record, all datasets were re-sampled first to a 20-yr
215 resolution (except for the sterol and stanol samples) and to a 60-yr resolution to include the sterol
216 and stanol samples. Breakpoint analysis was conducted on the slopes of the re-sampled datasets
217 using the “segmented” package in R version 3.3.3 (R Development Team; Muggeo, 2008).
218 The breakpoints that were common to both re-sampled datasets are reported. The 95%
219 confidence intervals were determined by calculating the pooled uncertainty from the breakpoint
220 analysis and age model.

221

222 *2.5 Leaf waxes as a proxy for vegetation change*

223 Shifts in vegetation were assessed by measuring changes in the *n*-alkane distribution.
224 Higher-level plants produce longer-chain *n*-alkanes (e.g., C₂₅-C₃₃), and can be used to further
225 differentiate grasses and shrubs, which typically produce higher concentrations of C₃₁ *n*-alkanes,
226 from woody plants (C₂₇ and C₂₉) based on differences in the average chain length (Cranwell,

227 1973; Maffei, 1996). Therefore, shifts in the average chain length (ACL) are often used to
228 reconstruct changes in vegetation as follows:

229

$$230 \text{ACL}_{27-33} = \sum \frac{C_i \times [C_i]}{[C_i]} \quad [2]$$

231

232 where $[C_i]$ represents the concentration of n -alkanes and C_i corresponds to the hydrocarbon
233 chain-length.

234

235 *2.6 Sterols and stanols as fecal biomarkers and indicators of lake water column redox conditions*

236 Sterols and stanols are structurally diverse and relatively stable compounds in the
237 geologic record, making them useful tracers of inputs and microbial activity in the sediment (e.g.
238 Nishimura & Koyama, 1977; Volkman, 1986; Leeming et al., 1996). For instance, C_{29} -sterols are
239 mainly produced by terrestrial plants and certain species of phytoplankton, whereas C_{27} -sterols
240 are derived from cholesterol and are therefore predominantly aquatic in origin (Nishimura &
241 Koyama, 1977; Huang & Meinschein, 1976, 1979; Volkman, 1986). $5\alpha(H)$ -stanols, however, are
242 present in low abundance in living organisms and are mainly derived from the microbial
243 reduction of Δ^5 -sterols in the sediment (Gaskell & Eglinton, 1975; Nishimura & Koyama, 1977;
244 Rieley et al., 1991). The conversion of Δ^5 -sterols to $5\alpha(H)$ -stanols is dependent on both the
245 contribution of autochthonous and allochthonous organic matter to the sediment and the redox
246 potential (Nishimura, 1977). The ratio of $5\alpha(H)$ -stanols/ Δ^5 -sterols can thus be used to track
247 changes in inputs and the redox potential, and is calculated as follows:

248

249
$$\frac{5\alpha(H)\text{-stanols}}{\Delta^5\text{-sterols}} = \frac{\text{cholestanol} + \text{campestanol} + \text{stigmastanol} + \text{sitostanol}}{\text{cholesterol} + \text{campesterol} + \text{stigmasterol} + \beta\text{-sitosterol}} \quad [3]$$

250

251 An increase in $5\alpha(H)$ -stanols/ Δ^5 -sterols indicates more reducing conditions in the sediment, and
252 also highlights the preferential degradation of Δ^5 -sterols relative to $5\alpha(H)$ -stanols in the sediment
253 (Gaskell & Eglinton, 1975; Nishimura, 1977; Nishimura & Koyama, 1977).

254 Certain 5β -stanols are produced in high abundance in the gastrointestinal tract of higher
255 mammals, making them biomarkers for fecal inputs from these organisms (Leeming et al., 1996).
256 For instance, carnivores and omnivores, particularly humans, consume large quantities of
257 cholesterol that gets microbially reduced to coprostanol (5β -cholestan- 3β -ol) and epi-coprostanol
258 (5β -cholestan- 3α -ol) by their gut microbiome (Leeming et al. 1996). Ruminants, on the other
259 hand, reduce a high proportion of plant sterols, e.g. sitosterol and stigmasterol, to 24-
260 ethylcoprostanol and 5β -stigmastanol, respectively (Leeming et al., 1996; Bull et al., 2002). A
261 high abundance of coprostanol, epi-coprostanol, 24-ethylcoprostanol, or 5β -stigmastanol relative
262 to background conditions, could indicate that humans and/or livestock were present in the
263 catchment area of a lake.

264

265 *2.7 Isoprenoidal glycerol dialkyl glycerol tetraethers (isoGDGTs) in lakes*

266 Isoprenoidal glycerol dialkyl glycerol tetraethers (isoGDGTs) are traditionally used as
267 proxies for sea surface temperatures but are also used in lake studies as indicators for specific
268 archaea (e.g. Sinninghe Damsté et al., 2009; Schouten et al., 2013). In particular, changes in lake
269 trophic state and dissolved oxygen content can drive shifts in archaeal communities that produce
270 isoGDGTs, making them useful tracers for paleo-ecological studies (e.g. Blaga et al., 2009;
271 Naeher et al., 2014).

272 Crenarchaeol (Cren) and its regioisomer, Crenarchaeol' (Cren') are specific to
273 *Thaumarchaeota*, or ammonia-oxidizers, in particular groups I.1a and I.1b (Sinninghe Damsté et
274 al., 2002, 2012; Pearson et al., 2004; Schouten et al., 2008; Pitcher et al., 2010, 2011). Group
275 I.1a is found in high abundance near the thermocline and nitrocline in lakes, and is associated
276 with the production of Cren and minor amounts of GDGT-0 and Cren' (Sinninghe Damsté et al.,
277 2002; Auguet et al., 2011, 2012; Pitcher et al., 2011; Buckles et al., 2013). Cren' is produced in
278 higher abundance by *Thaumarchaeota* group I.1b both in soils and in the water column (Pitcher
279 et al., 2010; Sinninghe Damsté et al., 2012; Buckles et al., 2013; Kumar et al., 2019).

280 Identifying different producers of GDGT-0 is more complex, as GDGT-0 can be
281 produced by methanogenic *Euryarchaeota* (Pancost et al., 2000), anaerobic methane-oxidizing
282 Archaea (Pancost et al., 2001; Wakeham et al., 2003), heterotrophic uncultured crenarchaeotal
283 groups (Buckles et al., 2013), and even *Thaumarchaeota* in low abundance (Sinninghe Damsté et
284 al., 2002, 2012; Pitcher et al., 2011). Anaerobic methane-oxidizing archaea can be distinguished
285 by a concurrent increase in the fractional abundance of GDGTs-0, -1, and -2 (Pancost et al 2001;
286 Wakeham et al, 2003), whereas methanogenic *Euryarchaeota* are dominated by GDGT-0 and
287 only minor amounts of GDGT-1 and -2, and no crenarchaeol (Pancost et al., 2000; Blaga et al.,
288 2009; Naeher et al., 2014).

289

290 **3. Results**

291 *3.1 Lacustrine sedimentary units*

292 Prior to c. 1000 CE the core is composed of light brown silty mud that is interspersed
293 with numerous erosive layers of poorly sorted pebbles and sand arranged in fining-upward grain-
294 size sequences that are most likely associated with mass-wasting events (Unit 1, Figure S4).

295 Between c. 1000-1450 CE the core consists of mud interbedded with six thin layers of sand and
296 one layer of gravel-sized clasts c. 1200 CE (Unit 2). The uppermost section of the core is
297 characterized by laminated sediments between c. 1450-2000 CE (Unit 3). The laminations
298 consist of darker lamina composed of silt and clay and lighter layers rich in diatoms. At the very
299 top of the core (c. 2000-2015 CE), there is a shift back to massive brown-black mud (Unit 4).

300

301 *3.2 Hydroclimate variability in the Azores*

302 The distribution of FAMES in the Lake Funda record is dominated by C₂₆ (850-1580 CE)
303 and C₂₈ (1581-1940 CE; Figure S5). A high fractional abundance of C₂₈ FAMES was previously
304 reported in a permanently stratified lake in Eastern Africa, and was attributed to the combined
305 input from terrestrial plant material and *in situ* production (van Bree et al., 2018). C₃₀ FAMES,
306 however, are predominantly sourced from terrestrial plants and were therefore targeted for
307 compound-specific hydrogen isotope measurements in this study.

308 In the δD_{wax} record of C₃₀ FAMES the variance is low ($\sigma^2 = 6 \text{ ‰}$) between c. 1000-1400
309 CE (Figure 2). Breakpoints at 1462 ± 14 CE and 1514 ± 13 CE correspond to a change from
310 more enriched to depleted values in δD_{wax} (Table 1). After c. 1400 CE, the variance in the δD_{wax}
311 values increases ($\sigma^2 = 16 \text{ ‰}$) with periods when δD_{wax} is depleted c. 1500-1620 and 1660-1860
312 CE and a period of enriched δD_{wax} values occurring c. 1880-1980 CE. A sharp depletion from c.
313 1980-1995 CE is followed by enriched δD_{wax} values after c. 2000 and a return to more depleted
314 values c. 2010 CE.

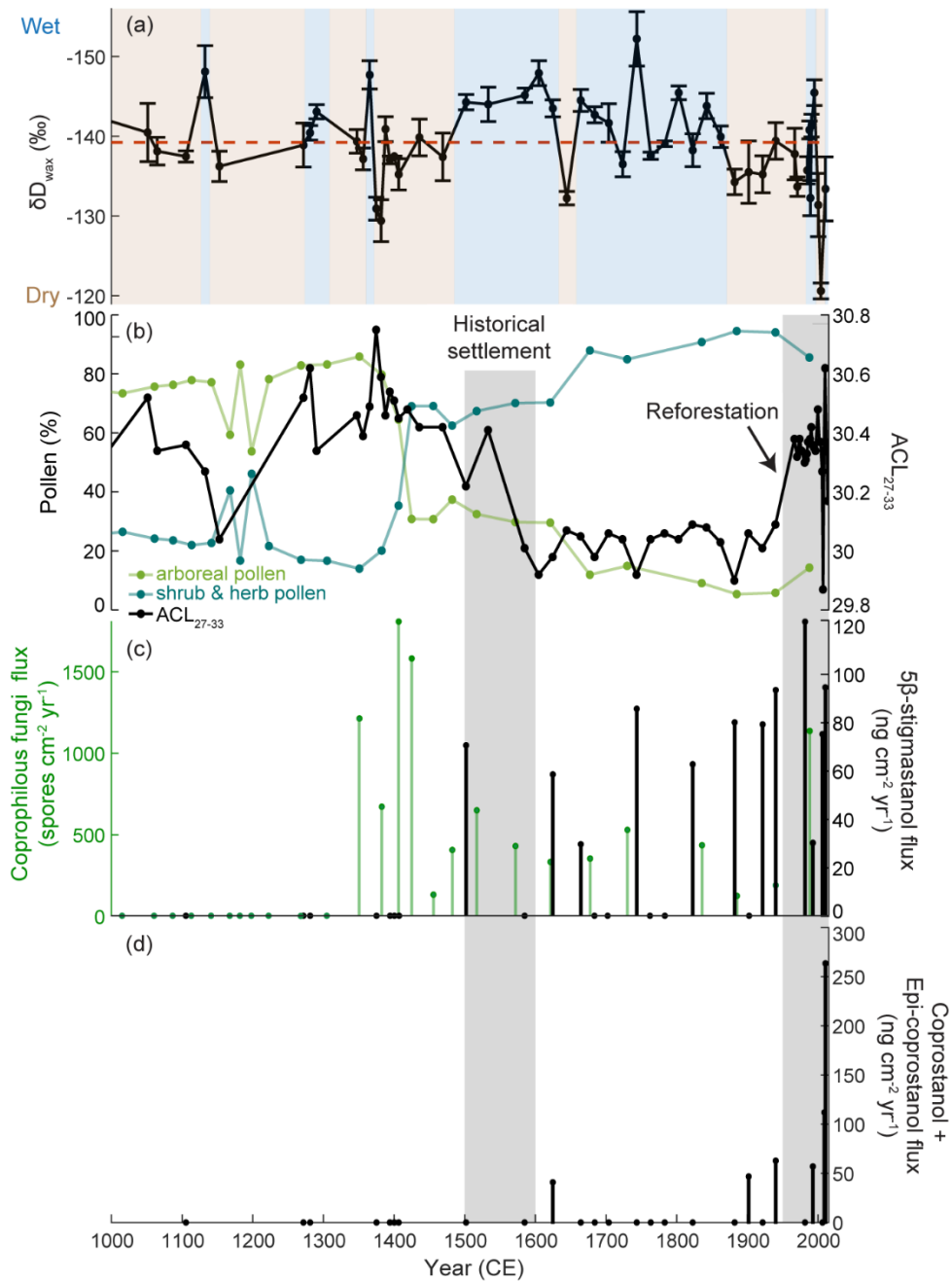


Figure 2. (a) Changes in hydroclimate are noted by shifts in FAMES C_{30} δD_{wax} , where more depleted isotopes correspond to wetter conditions and enriched isotopes correspond to drier conditions (the dashed red line corresponds to the mean of the dataset). Intervals where the climate was wetter or drier are denoted by blue and brown bars, respectively. Major changes in vegetation composition are noted by shifts in (b) ACL_{27-33} and are compared with results arboreal (green) and shrub and herb (blue) pollen data (Raposeiro et al., 2021a; Ritter et al., 2022). Fecal biomarkers, including (c) coprophilous fungal spores (green) and 5β -stigmastanol (black) and (d) coprostanol and epi-coprostanol (Raposeiro et al., 2021a; Ritter et al., 2022), are used to determine when livestock and humans were present in the catchment area. The first gray bar marks the first signs of human activities in the 16th century, and the second gray bar indicates when reforestation efforts started c. 1950 CE.

316 3.3 Changes in sediment composition and geochemistry

317 Before c. 1300 CE, C/N values are about 18 but then decrease between 1319 ± 36 CE
318 and 1602 ± 16 CE to about 10 (Figure 3 & Table 1). Biogenic silica (BSi) increases after $1314 \pm$
319 33 CE and plateaus after 1372 ± 47 CE. This change coincides with an abrupt decrease in $\delta^{15}\text{N}$
320 at 1343 ± 37 CE and a further decrease between 1492 ± 11 CE and 1671 ± 8 CE (Figure 3).
321 There is also a gradual decrease in $\delta^{13}\text{C}$ values after 1570 ± 14 CE (Figure 4).

322

323 3.4 Changes in the lake catchment and lake redox conditions

324 To infer specific changes in the lake catchment, ACL₂₇₋₃₃ is used to track changes in the
325 vegetation composition and sterols and stanols are used as proxies for the local presence of
326 livestock and humans and as an indicator of changing redox conditions in the lake sediment.
327 Breakpoints for ACL₂₇₋₃₃ at 1386 ± 39 CE and 1582 ± 12 CE mark a shift towards a decreasing
328 trend in ACL₂₇₋₃₃ (Figure 2 & Table 1). Unfortunately, we do not have access to native and
329 endemic plants from the Azores to determine the *n*-alkane signatures, so we interpret the
330 decrease in *n*-alkane distribution to reflect a decrease in native gymnosperms based on surveys of
331 alkane distributions in global vegetation (Diefendorf et al., 2011). This interpretation is
332 consistent with palynological data indicating a decrease in *Juniperus brevifolia* (Seub.) Antoine
333 and *Picconia azorica* (Tutin) Knobl and a gradual increase of native grasses (Poaceae) and
334 shrubs (e.g. *Erica azorica* Hochst. ex Seub and *Myrsine*) in the pollen record (Connor et al.,
335 2012; Raposeiro et al., 2021a, b). The flux of sterols and stanols increases between c.1200-1500
336 CE, except for coprostanol, epi-coprostanol, and 5β -stigmastanol (Figure S6). 5β -stigmastanol
337 first occurs c. 1500 CE, but does not become frequent in the sediment record until after c. 1620
338 CE (Figure 2). There is one occurrence of coprostanol c. 1620 CE, however, coprostanol and epi-

339 coprostanol do not become abundant in the sediment record until after c. 1900 CE. An increase
 340 in sterols and stanols relative to TOC occurs after c. 1400 CE (Figure S7). This coincides with an
 341 increase in $5\alpha(H)$ -stanols/ Δ^5 -sterols after 1481 ± 20 CE and a continued increase in this ratio
 342 until the present (Figure 4). ACL_{27-33} values increase again after 1943 ± 9 CE.

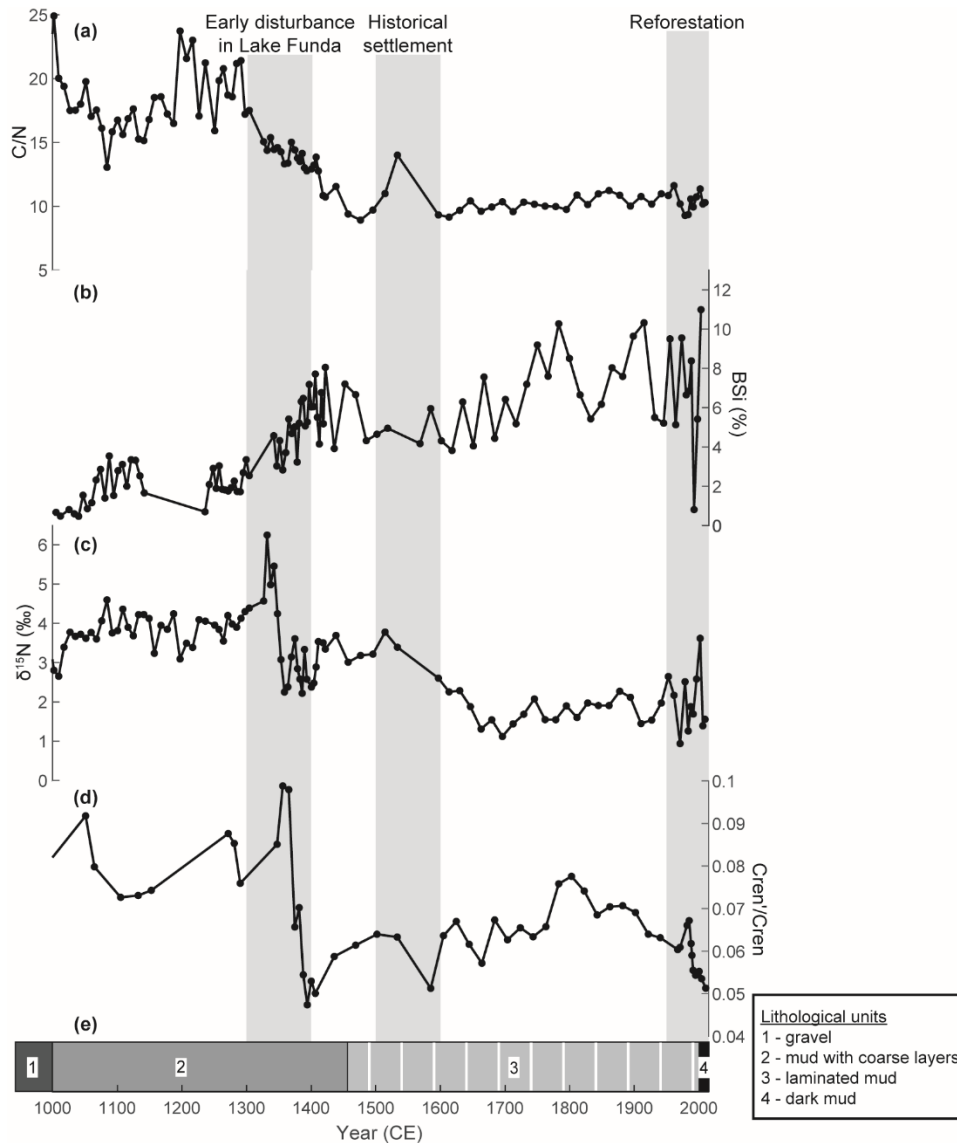
343

344 **Table 1.** Segmented breakpoint analysis for the proxy records discussed in this study with the pooled uncertainty
 345 shown. The direction of change indicates whether the proxy value increased (+), decreased (-), or did not change (no
 346 change).

347

	Proxy	Segmented Breakpoint Analysis		Direction of Change
		Year (CE)	95% CI (\pm)	
Climate	δD_{wax} C ₃₀ FAMES (‰)	1462	14	- (depleted)
		1514	13	+ (enriched)
Catchment area	ACL_{27-33}	1386	39	-
		1582	12	No change
		1943	9	+
Organic matter sources & lake biogeochemical cycles	C/N	1319	36	-
		1602	16	No change
	BSi (%)	1314	33	+
		1372	47	+
	$\delta^{15}N$ (‰)	1343	37	-
		1388	36	+ / No change
		1492	11	-
		1671	8	No change
	Cren/Cren	1352	39	-
1421		13	+	
1868		12	-	
GDGT-0/Cren	1544	15	+	
	1634	15	+	
	$\delta^{13}C$ (‰)	1570	14	- (depleted)
Redox conditions	$5\alpha(H)$ -stanols/sterols	1481	20	+

348



349
 350 **Figure 3.** Changes in organic matter inputs to the lake are noted by shifts in (a) C/N and are compared with (b)
 351 changes in diatom productivity, BSi (%). Further changes in the lake are noted by (c) δ¹⁵N and (d) Cren'/Cren
 352 corresponds to changes in the *Thaumarchaeota* community. (e) Distinct changes in the sediment core are noted by
 353 the different lithological units. The first gray bar indicates coincident changes in the sediment record. The second
 354 gray bar corresponds to the historical settlement of Flores Island in the 16th century and the final gray bar
 355 corresponds to recent reforestation efforts (c. 1950 CE to the present).
 356

357 *3.3 isoGDGTs as tracers of biogeochemical cycles in the lake water column*

358 In Lake Funda, the composition of isoGDGTs identified in the sediment are distinctly
 359 different from the isoGDGT composition of the soils in the catchment, indicating that most of the
 360 isoGDGTs in the sediment are produced in the water column (Figure S8). Throughout the

361 sediment record GDGT-0 is present in higher abundance relative to other isoGDGTs, and Cren
 362 and Cren' are both present throughout the record. Two distinct breakpoints occur in the isoGDGT
 363 composition: a decrease in Cren'/Cren between 1352 ± 39 CE and 1421 ± 13 CE and an
 364 increase in GDGT-0/Cren about 1544 ± 15 CE (Figure 3 & 4). The later increase in GDGT-0
 365 relative to Cren also coincides with a decrease in GDGTs-1 and -2 (Figure S8).
 366

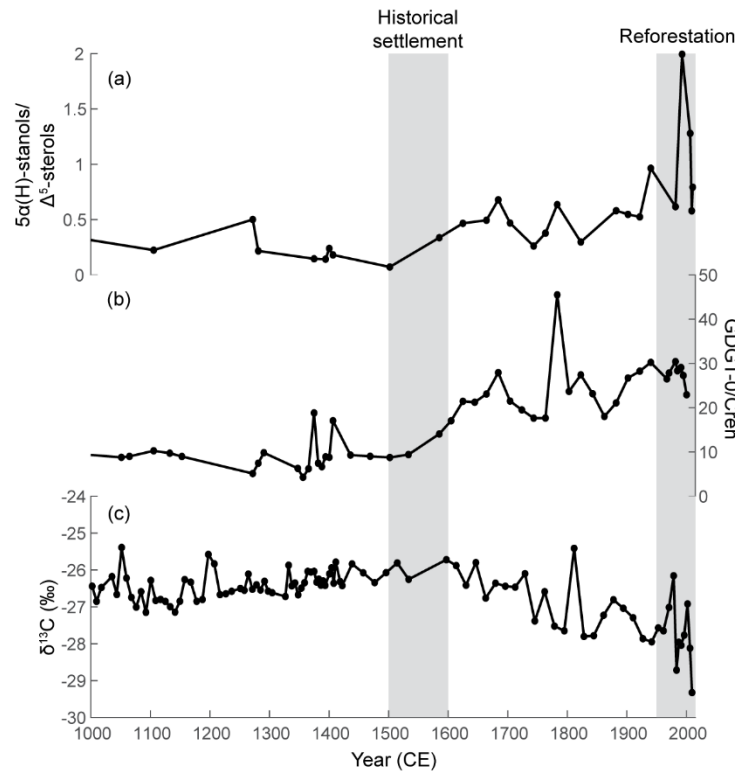


Figure 4. Redox conditions in the lake bottom water are noted by changes in (a) $5\alpha(H)$ -stanols/ Δ^5 -sterols. Similarly, (b) GDGT-0/Cren reflects changes in lake bottom water processes and changes in (c) $\delta^{13}C$ are shown for comparison. The gray bars correspond to when human activities were first detected in the catchment area in the 16th century and the reforestation efforts that began c. 1950 CE.

367 4. Discussion

368 4.1 Controls on leaf wax hydrogen isotopes in the Azores

369 The hydrogen isotope composition of leaf waxes (δD_{wax}) in higher terrestrial plants (i.e.
370 C_{28} - C_{32} *n*-acids) is correlated with changes in δD of precipitation (δD_{precip} ; Sachse et al., 2012).
371 The variability in δD_{precip} reflects a combination of processes, including precipitation amount,
372 water source, transport history, and Rayleigh-type processes related to evaporation and
373 condensation (Craig, 1961; Dansgaard, 1964; Sachse et al., 2012). In the Azores changes in
374 precipitation amount, and also δD_{precip} , are dominated by shifts in the high-pressure Azores
375 anticyclone, resulting in both intra- and interannual variability associated with the North Atlantic
376 Oscillation (NAO; Hurrell, 1995; Santos et al., 2004; Cropper & Hanna, 2014; Hernández et al.,
377 2016). In the Azores, mean monthly event-based δD_{precip} from 1963-2014 is negatively correlated
378 with precipitation amount during the drier spring (MAM, $r = -0.72$, $p < 0.01$) and summer (JJA, r
379 $= -0.49$, $p < 0.05$) months and wetter fall (SON, $r = -0.41$, $p < 0.05$) season (Table 2; Global
380 Network of Isotopes in Precipitation (GNIP); Rubio de Inglés, 2016). The majority of vapor
381 mass originates from the tropical and sub-tropical regions of the Atlantic (including the Gulf of
382 Mexico), however, the vapor mass that reaches the Azores Archipelago receives additional vapor
383 inputs over the North Atlantic Ocean such that the isotopic variability associated with source
384 changes does not have a major impact on δD_{precip} (Araguás-Araguás et al., 2000; Gimeno et al.,
385 2010; Rubio de Inglés, 2016). In addition, a temperate oceanic climate leads to small variations
386 in air temperature on Flores, with average temperatures ranging from 15°C during the winter
387 months (DJF) to 23°C during the summer (JJA), and has a minimal influence on δD_{precip}
388 (Dansgaard, 1964; Baldini et al., 2008; Rubio de Inglés, 2016; Global Historical Climatology

389 Network (GHCN)). Therefore, we infer that the δD_{wax} of higher terrestrial plants is primarily
 390 influenced by changes in precipitation amount.

391
 392 **Table 2.** Spearman rank correlation coefficients comparing mean monthly air temperature and precipitation amounts
 393 with event-based δD_{precip} . The instrumental data is obtained from Ponta Delgada (1963-2014; Hernández et al., 2016;
 394 Global Network of Isotopes in Precipitation (GNIP)).
 395

	Air Temperature vs. δD_{precip}		Precipitation amount vs. δD_{precip}	
	<i>r</i>	<i>p</i>	<i>r</i>	<i>p</i>
Winter (DJF)	-0.09	0.63	-0.35	0.07
Spring (MAM)	0.30	0.14	-0.72	<0.01
Summer (JJA)	-0.07	0.74	-0.49	<0.05
Fall (SON)	0.13	0.51	-0.41	<0.05

396

397

398 *4.2 Impacts of early human activities on Lake Funda (c. 1000-1400 CE)*

399 The Portuguese are thought to have discovered and settled the Azores in the 15th century
 400 (Crosby, 2004). However, the Canary Islands, and possibly the Azores and Madeira, were
 401 already known to the Romans (c. 500 BCE) and Isidor de Sevilla (c. 600 CE), and in the 14th
 402 century the Azores Archipelago was included on maps and in atlases (Schäfer, 2003; Crosby,
 403 2004; see Raposeiro et al., 2021b). Paleoecological records from two Azorean islands (Corvo
 404 and Pico), show an almost simultaneous increase of fire-related proxies (e.g. charcoal particles
 405 and polycyclic aromatic hydrocarbons) and fecal biomarkers (e.g. 5 β -stigmastanol and
 406 coprophilous fungal spores) suggesting that humans first arrived in the archipelago between c.
 407 700-850 CE (Raposeiro et al., 2021b). Thus, it is likely that, at the very least, limited or
 408 temporary settlements existed well before the 15th century.

409 Between c. 1000-1500 CE there are very few changes in the ACL₂₇₋₃₃ record, and pollen
 410 data indicates that dense laurel forests dominated the catchment of Lake Funda (Connor et al.,
 411 2012; Raposeiro et al., 2021b). In addition, the δD_{wax} record from Lake Funda is characterized by

412 low variability and relative D-enrichment between c. 1000-1400 CE, suggesting that the climate
413 was relatively dry and stable (Figure 2). This coincides with overall drier conditions in Morocco
414 (c. 1000-1400 CE; Esper et al., 2007; Wassenburg et al., 2013; Ait Brahim et al., 2017) and the
415 Iberian Peninsula (c. 900-1300 CE; Sánchez-López et al., 2016). Similarly, results from the
416 Community Earth System Model (CESM-CAM5_CN) Last Millennium Ensemble transient
417 simulation suggest that early settlers encountered overall drier and warmer climate conditions
418 between c. 800 CE and the onset of the Little Ice Age (c. 1350-1450 CE; Raposeiro et al.,
419 2021b).

420 A decrease in C/N values and an increase in BSi after c. 1300⁺³²₋₂₈ CE corresponds to a
421 transition from terrestrially dominated to aquatically sourced organic matter inputs and
422 heightened productivity (Figure 3; Raposeiro et al., 2021b). A decrease in Cren'/Cren (Figure 4)
423 could also be a result of heightened primary productivity as ammonium concentrations increase
424 in the water column from the decomposition of particulate organic matter (Blaga et al., 2011;
425 Auguet et al., 2011, 2012; Kumar et al., 2019). This could promote increased ammonia oxidation
426 by *Thaumarchaeota* Group I.1a at the oxycline/thermocline and nitrocline, resulting in increased
427 Cren production relative to Cren' (Sinnighe Damste et al., 2009; Auguet et al., 2011, 2012; Blaga
428 et al., 2011; Kumar et al., 2019). The depletion in $\delta^{15}\text{N}$ at c. 1350⁺⁴⁴₋₃₄ CE differs from the
429 expected enrichment of $\delta^{15}\text{N}$ that is usually associated with increased primary productivity and a
430 decrease of terrestrial material (Hodell & Schelske, 1998; Brenner et al., 1999; Meyers et al.,
431 2003). The depletion in $\delta^{15}\text{N}$ occurs shortly after the first appearance of coprophilous fungal
432 spores (i.e., *Sporormiella*, *Sordaria*, and *Podospora*) c. 1350⁺⁴⁴₋₃₄ CE. We infer that the depletion
433 in $\delta^{15}\text{N}$ reflects an increase in N-fixation, which could result from the presence of livestock in the
434 catchment area that led to an increase of phosphorous inputs to Lake Funda (Raposeiro et al.,

435 2021b). Many lakes in the Azores, including Lake Funda, are phosphorus limited and increased
436 phosphorus inputs to the lake from livestock could lead to increased N₂-fixation by
437 cyanobacteria, lower $\delta^{15}\text{N}$ values, and promote eutrophication (Brenner et al., 1999; Meyers,
438 2003; Cruz et al., 2015; Raposeiro et al., 2021b).

439 The lack of 5 β -stigmastanol in our record despite the increase in fungal spores at this
440 time could reflect differences in the preservation, transport, or deposition of fungal spores
441 relative to fecal stanols (Guillemont et al., 2017; Zocatelli et al., 2017). Fungal spores are local
442 indicators of megaherbivores that can be transported via run-off or wind across 25-100 m (Gill et
443 al., 2013; Perrotti & van Asperen, 2019), and further transported on and within the lake. The
444 water-solubility of 5 β -stanols is low and they are typically bond to clays and particulate organic
445 matter, so their input to lake sediments is limited to run-off and riverine inflows (Walker et al.,
446 1982; Lloyd et al., 2012). In the case of Lake Funda, the steep catchment makes the lake difficult
447 to access, so humans and/or livestock likely only sought out the lake during drier climate
448 conditions, e.g. between c. 1300-1350 CE and c. 1370-1390 CE, and that the influx of 5 β -stanols
449 to the lake is likely reduced relative to fungal spores. For comparison, Lake Caldeirão is shallow
450 lake on Corvo Island is located in a wide crater with gentle slopes, making the lake easily
451 accessible to humans and livestock. In the present-day, livestock can be found at the edge of the
452 lake year-round. A higher concentration of both fecal stanol and coprophilous fungal spores
453 likely reach the lake sediment via run-off, which would explain the similar trends observed in the
454 fecal stanol and coprophilous fungal spore records from c. 700-850 CE to the present (see
455 Raposeiro et al., 2021b). In contrast, Lake Peixinho on Pico Island (870 m a.s.l) is more exposed
456 to the elements and is located at a higher altitude than Lake Funda (351 m a.s.l.) and Caldeirão
457 (410 m a.s.l.), such that fungal growth is likely limited by colder temperatures or the fecal

458 material is washed away before the fungus has enough time to germinate (Dickinson &
459 Underhay, 1977; Wood & Wilmshurst, 2012; Perrotti & van Asperen, 2019). In this case, we
460 might observe a higher influx of 5β -stanols relative to fungal spores, which might explain the
461 early appearance of 5β -stanols (c. 700-850 CE) and the lack of fungal spores until c. 1100 CE in
462 Lake Peixinho (see Raposeiro et al., 2021b).

463 The increase in nutrient inputs to Lake Funda occurred during stable and drier conditions,
464 as indicated by the low variance and enriched values of δD_{wax} , on Flores Island and without
465 changes in the catchment or noticeable changes in the sediment core. Although there are no
466 significant changes in vegetation composition nor evidence of changes in soil erosion, the
467 introduction of livestock could enhance nutrient cycling in the landscape and result in more open
468 patches of vegetation leading to increased nutrient leaching from soils into the lake from the
469 catchment (e.g. McNaughton et al., 1997). This is also observed in other islands of the Azores
470 Archipelago as well as the Faroe Islands and Iceland, where the introduction of livestock resulted
471 in increased nutrient loading and changes in lake trophic state before noticeable changes in soil
472 erosion and vegetation composition occurred (Hannon et al., 2005; Lawson et al., 2007;
473 Raposeiro et al., 2021b).

474 If early settlements were present on Flores Island, then they were likely abandoned before
475 the 15th century as there are no records of humans living on the island when the first Portuguese
476 explorers and later Flemish and Portuguese settlers arrived in the mid-15th and early 16th century
477 (Raposeiro et al., 2021b). However, the continued decrease in C/N values until c. 1500 CE
478 suggests that Lake Funda was still adjusting to the initial disturbance. Thus, the initial increase in
479 primary productivity in Lake Funda could be evidence of human impacts on the island prior to

480 the accepted settlement of Flores Island and likely made the lake ecosystem more susceptible to
481 later disturbances in the lake catchment.

482

483 *4.2 Environmental impacts of human settlements on Flores Island (c. 1401-1900 CE)*

484 The start of organized Portuguese explorations along the western coast of Africa began in
485 the late 14th to early 15th century (Meneses, 2009) during a drier (enriched δD_{wax} values in the
486 Funda record) climate interval on the Flores Island. Similarly, relatively low lake levels recorded
487 on Pico Island and São Miguel suggest that the climate was overall drier in the Azores
488 Archipelago during the 15th century (Björck et al., 2006; Hernández et al., 2017). After 1432 CE
489 the Portuguese established settlements in Santa Maria and São Miguel, and eventually Flemish
490 settlements were established on Flores Island in 1472 CE but were abandoned after a few years
491 (Schäfer, 2003; Connor et al., 2012; Rull et al., 2017; Raposeiro et al., 2021b). More extensive
492 settlement of Flores Island by the Portuguese began c. 1510 CE during a wetter climate interval
493 recorded by more depleted δD_{wax} values in the Lake Funda record (Lages, 2000; Schäfer, 2003;
494 Connor et al., 2012). Lake-levels in waterbodies on São Miguel, however, continue to decrease
495 after c. 1500 CE (Hernández et al., 2017) and more frequent negative phases in the NAO during
496 the winter season suggest that drier conditions prevailed (Raposeiro et al., 2021b). In this
497 context, the more depleted δD_{wax} values, reflecting wetter conditions, observed in Lake Funda
498 could be attributed to differences in precipitation seasonality. The δD_{wax} record from Flores
499 Island primarily reflects spring and summer precipitation during the period of leaf wax
500 production (Tipple et al., 2012), when we observe the strongest correlation between δD_{precip} and
501 rainfall amount (see Table 2). In contrast, changes in lake-level reflect mean annual changes in

502 precipitation and the NAO is primarily responsible for the variability in winter precipitation
503 (Hernández et al.2016).

504 Despite the relatively recent settlement of the islands, the present-day landscape has been
505 completely altered and it is uncertain how vulnerable this has made the current island ecosystems
506 to climate change (e.g. Antunes & Rodrigues, 2011; Connor et al., 2012; Cruz et al., 2015; Rull
507 et al., 2017). The more frequent occurrence of 5 β -stigmastanol after c. 1620 CE in the Lake
508 Funda record likely reflects the widespread release of livestock on the islands to provide food for
509 settlers (Figure 2; Schäfer, 2003; Smith, 2010). This was a common practice among the
510 Portuguese as they settled Macaronesia, for instance, in Cabo Verde the timing of human
511 settlement (c. 1450-1600 CE) coincides with an abrupt increase in non-obligate coprophilous
512 fungi from livestock feces, followed by the gradual proliferation of newly introduced flora and
513 increased erosion (c. 1600-1700 CE; Castilla-Beltrán et al., 2019). Most settlements on Flores
514 were established in low coastal areas (Raposeiro et al., 2021b), which could explain the lack of
515 coprostanol and epi-coprostanol in the lake sediments until the 20th century during a prolonged
516 dry interval as indicated by more enriched δD_{wax} values. On Flores Island, the introduction of
517 livestock coincides with a decrease in ACL₂₇₋₃₃ between c. 1500-1600 CE, as native vegetation
518 (i.e., *Juniperus brevifolia* and *Picconia azorica*) was cleared to create a more open landscape for
519 livestock (Connor et al., 2012; Raposeiro et al., 2021b). Similarly, in the Canary Islands, early
520 European settlers cleared forests in the lowlands for agriculture and pastures for livestock (de
521 Nascimento et al., 2009). The decrease in ACL₂₇₋₃₃ that is associated with deforestation on Flores
522 Island is in direct contrast to the increase in ACL₂₅₋₃₁ that is observed on Iceland as Norse settlers
523 cleared birch trees (Richter et al., 2021). Higher ACL₂₇₋₃₃ values in Flores could be associated
524 with increased production of longer chain *n*-alkanes by plant species in the family *Juniperus*

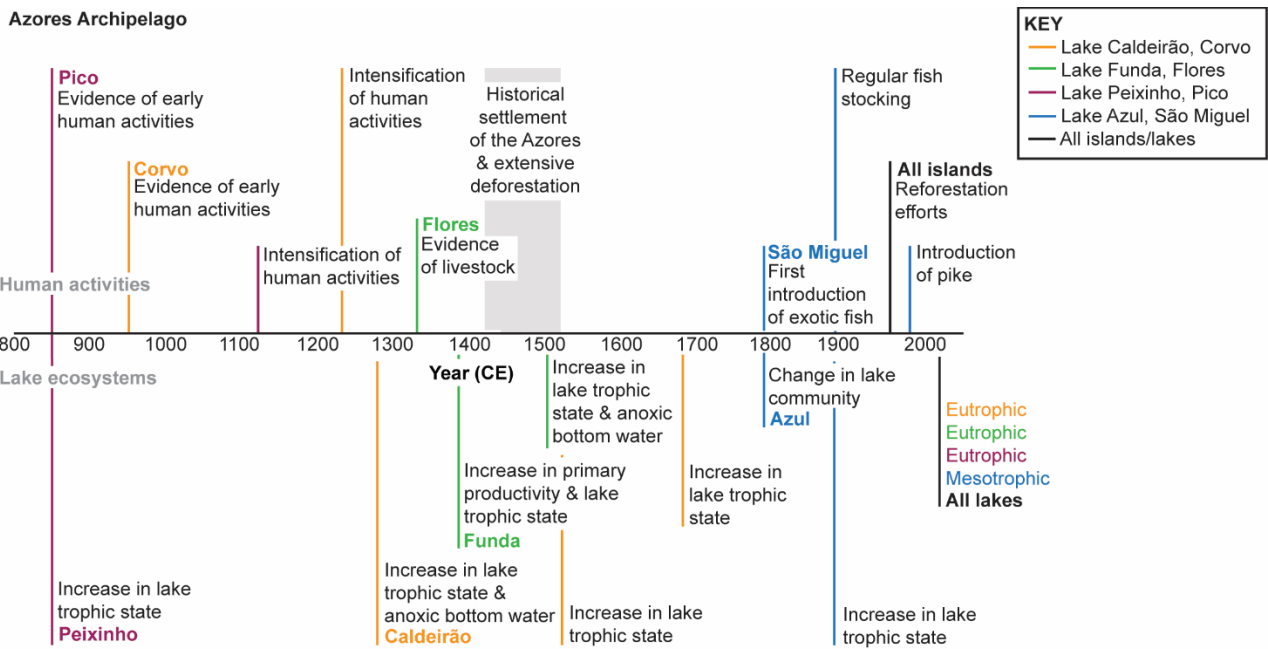
525 (C₃₃-C₃₅; Diefendorf et al., 2011), whereas birch trees (*Betula pubescens* and *Betula nana*) in
526 Iceland predominantly produce shorter chain *n*-alkanes (C₂₅-C₂₇; Schwark et al, 2002; Balascio
527 et al. 2018).

528 The effects of Portuguese activities on Lake Funda are apparent beginning about c.
529 1500⁺¹⁰₋₁₁ CE when laminations rich in diatoms are visible in the sediment record, suggesting that
530 increased nutrient availability led to heightened primary productivity and a further decrease in
531 $\delta^{15}\text{N}$ (Figure 3). At this time, however, we also observe a shift to more reducing conditions in the
532 sediment, i.e. an increase in $5\alpha(H)$ -stanols/ Δ^5 -sterols, c. 1500-1550 CE from oxygen depletion in
533 the water column (Figure 4; Gaskell & Eglinton 1975; Nishimura, 1977; Nishimura & Koyama,
534 1977; Kalff, 2002). In addition, increases in GDGT-0/Cren and a decrease in GDGT-1 and -2
535 suggest the production of isoGDGTs by methanogenic archaea in the bottom water of the lake
536 (Figure S7; Pancost et al., 2000; Blaga et al., 2009; Naeher et al., 2014). This is supported by the
537 gradual decrease in bulk $\delta^{13}\text{C}$ values after c. 1570 CE as more depleted carbon is added to the
538 epilimnion from increased methanogenesis (e.g. Hollander & Smith, 2001).

539 Increased primary production and evidence of hypoxic conditions in the lake bottom
540 water suggest that Lake Funda underwent a relatively rapid period of nutrient addition, loss of
541 bottom-water oxygen, and thus eutrophication that occurred as land clearance became
542 widespread in c. 1500 CE. In contrast, Lake Azul on São Miguel responded more gradually to
543 human impacts in the catchment area with the lake remaining relatively pristine and oligotrophic
544 until the introduction of exotic fish in the 1800s (Figure 5; Raposeiro et al., 2017). A rapid
545 response in lacustrine ecosystems to human activities is observed during the settlement of
546 Iceland and the Faroe Islands, but less so in Greenland (Hannon et al., 2005; Lawson et al., 2005,
547 2007; Massa et al., 2012; Richter et al., 2021). Cultural eutrophication in Lake Funda after c.

548 1500 CE could reflect a loss of resilience as the lake ecosystem reached a tipping point from
549 repeated disturbances in the catchment (i.e., human activities in c. 1300 CE and c. 1500 CE)
550 and/or an intensification of human activities after c. 1500 CE (Ritter et al., 2022). Such a tipping
551 point could be driven by increased nutrient availability that trigger positive feedbacks between
552 eutrophication, bottom water oxygenation, and internal loading of P (Scheffer, 1998; Marsden,
553 1989). We infer that historic and continued nutrient inputs from the landscape and potential
554 internal phosphorous-loading due to hypolimnetic deoxygenation during the summer months led
555 to an alternative stable state in Lake Funda (Scheffer et al., 2001). A similar loss of resilience
556 from early human activities is observed in lakes in Canada, Greenland, and Switzerland, where
557 even after the settlements were abandoned the lakes remained eutrophic or, if they did recover,
558 were more susceptible to later disturbances (Douglas et al., 2004; Ekdahl et al., 2004; Hillbrand
559 et al., 2014).

560 Despite a shift to more variable and wetter conditions between c. 1660-1860 CE,
561 indicated by more depleted δD_{wax} values, the vegetation composition (ACL_{27-33}) stabilized
562 between c. 1600-1950 CE in the catchment area of Funda (Figure 2). However, $5\alpha(H)$ -
563 stanols/ Δ^5 -sterols and GDGT-0/Cren values continued to increase during this time period, which
564 would suggest that eutrophic conditions in Lake Funda were sustained by hysteresis in the
565 system.



566

567 **Figure 5.** A timeline highlighting major human activities on four different Azorean islands and ecological changes
 568 that occurred in four different lakes on these islands (figure based on data from Raposeiro et al., 2017, 2021b).

569

570 *4.3 Ecological changes in the Azores in the 20th and 21st centuries (c. 1901-2015 CE)*

571 The transition from the 19th to early 20th century was marked by major environmental and
 572 climatic changes in broader Macaronesia. In Flores, δD_{wax} values remain enriched relative to the
 573 mean from c. 1880-1980 CE with a slight depletion from c. 1940-1970 CE followed by a sharper
 574 depletion between c. 1980-1995 CE, indicating an overall drier climate until c. 1940 CE
 575 followed by a gradual increase in precipitation that peaks c.1980-1995 CE. This is reflected by
 576 the gradual increase in precipitation between 1943-2012 recorded in instrumental data from
 577 Ponta Delgada, São Miguel (Hernández et al., 2016). However, we do observe a return to drier
 578 conditions near the beginning of the 21st century, which could reflect several anomalous years
 579 with drier conditions on both Flores Island and São Miguel from 1999-2000 CE and 2003-2005
 580 CE before a return to wetter conditions between 2006-2015 CE (Hernández et al., 2016; Global
 581 Historical Climatology Network (GHCN)).

582 A sharp increase in ACL₂₇₋₃₃ values c. 1950 CE in Lake Funda (Figure 2) marks the start
583 of major reforestation efforts, as the local Forestry Service began to actively plant *Cryptomeria*
584 *japonica* in the Azores (Rull et al., 2017; Borges et al., 2019). Similarly, in Cabo Verde exotic
585 trees, such as *Pinus* and *Acacia*, were introduced in the early 20th century to help reduce land
586 degradation (Castilla-Beltrán et al., 2019). The combination of a drier climate and more trees in
587 the lake catchment area in the early 20th century should act to stabilize the soil, which in theory
588 should lead to reduced erosion and external nutrient loading and therefore lower primary
589 productivity and improve oxygenation in the water column. In Lake Funda the lack of changes in
590 $5\alpha(H)$ -stanols/ Δ^5 -sterols and GDGT-0/Cren suggest that there was little change in the microbial
591 community response to changes in erosion and nutrient loading (Figure 4). Limnological surveys
592 over the last two decades confirm that eutrophication continues to be a problem for Lake Funda
593 and hypoxic, and sometimes fully anoxic, conditions develop in the lake bottom water during the
594 summer and fall months (Figure S1 & S2). Continued internal loading of phosphorus and other
595 changes in the nitrogen and carbon cycle could promote the increase in microbially mediated
596 hydrogenation of Δ^5 -sterols to $5\alpha(H)$ -stanols and methanogenesis in the bottom water that we
597 observe in Lake Funda (Gaskell & Eglinton 1975; Nishimura, 1977; Nishimura & Koyama,
598 1977; Kalff, 2002).

599 Eutrophication is a problem for numerous lakes in the Azores Archipelago, and as
600 exemplified by this case study in Lake Funda and several other paleoecological studies in the
601 Azores, these changes in trophic state can be attributed to past human land use changes and/or
602 the introduction of fish (Figure 5; Skov et al., 2010; Antunes & Rodrigues, 2011; Cruz et al.,
603 2015; Raposeiro et al., 2017). Although external nutrient loads were reduced in Lake Furnas and
604 Sete Cidades (Lake Azul and Lake Verde) on São Miguel, nitrate and phosphorus concentrations

605 in the lakes remain high from N₂-fixation and internal P-loading during the summer months,
606 respectively (Cruz et al., 2015). Lake Funda is faced with a similar scenario, where
607 eutrophication is sustained from internal loading and suggests that more aggressive remediation
608 strategies are needed for the lake ecosystem to recover (Schindler, 2006). In contrast to some of
609 the lacustrine ecosystems in the high North Atlantic (e.g. Iceland, Faroe Islands, and Greenland),
610 Lake Funda underwent what appears to be a permanent shift in trophic state in response to
611 human activities in the landscape (Lawson et al., 2005, 2007; Massa et al., 2012; Richter et al.,
612 2021). Even though settlements were never established in the catchment of Lake Funda, early
613 human activities likely made the lake more susceptible to later disturbances. Our study highlights
614 the importance of understanding early human impacts and the natural state of lake ecosystems, as
615 this can have a large influence on the current trophic state of lakes and the remediation strategies
616 needed to tackle the problem.

617

618 **5. Conclusions**

619 Prior c. 1400 CE, climate on Flores Island was characterized by overall drier and more
620 stable conditions. During the 14th century, increases in primary productivity within Lake Funda
621 indicate a response to heightened nutrient loading from the catchment in response to the earlier
622 arrival of humans on Flores Island. The documented settlement of the Azores Archipelago during
623 the 15th to 16th centuries occurred at the start of the LIA during a prolonged wet period in Flores
624 Island. Increased precipitation most likely contributed to earlier abandonments of settlements on
625 Flores Island between 1452-1510 CE before the establishment of permanent settlements after c.
626 1510 CE (Lages et al., 2009). Increases in 5 β -stigmastanol and a rapid decrease in ACL₂₇₋₃₃ in
627 the 16th century, point to the widespread introduction of cattle and clearance of native vegetation,

628 respectively, on Flores Island by the Portuguese. Increased nutrient inputs to Lake Funda
629 resulted in a permanent shift in the lake trophic state as marked by a further increase in primary
630 productivity and the onset of hypoxic conditions in the lake bottom water. Despite recent
631 reforestation efforts to reduce soil erosion, Lake Funda has remained eutrophic either from
632 sustained nutrient inputs or internal loading of phosphorus. Many of the environmental issues in
633 the Azores are likely to be exacerbated by a warming climate and changes in precipitation. For
634 instance, warming temperatures can lead to prolonged lake stratification that could further
635 exacerbate already eutrophic systems (Woolway & Merchant, 2019). Environmental
636 management strategies need to account for the potential impacts this might have on already
637 vulnerable lake ecosystems.

638

639 **Data Availability**

640 The age model for this core, the total carbon and nitrogen data, the bulk carbon and nitrogen
641 isotopes, the sterol and stanol abundances, and biogenic silica data are available at Raposeiro et
642 al. (2021a; <https://doi.pangaea.de/10.1594/PANGAEA.933712>). Additional data published in
643 this manuscript are available at Richter et al. (2022; <https://doi.org/10.1594/PANGAEA.941316>).

644

645 **Acknowledgements**

646 This work was supported by RapidNAO (CGL2013-40608-R), PaleoModes (CGL2016-75281),
647 DiscoverAzores (PTDC/CTA AMB/28511/2017), a Luso-American Foundation “Crossing the
648 Atlantic” grant, the Netherlands Earth Systems Science Center, the Institute at Brown for
649 Environment and Society, and the Geological Society of America. Support for undergraduate
650 research was provided by the Brown University Undergraduate Teaching & Research Awards.

651 We would like to thank everyone who participated in the 2017 and 2018 field campaigns to the
652 Azores, in particular A. C. Costa and E. Zettler. We would like to thank J.S. Sinninghe Damste
653 for support and advice. We would also like to thank J. Orchardo, E. Santos, and M. Baas for
654 technical support and advice, and R. Vachula for advice.

655

656 **References**

657 Ait Brahim, Y., Cheng, H., Sifeddine, A., Wassenburg, J.A., Cruz, F.W., Khodri, M., Sha, L.,

658 Pérez-Zanón, N., Beraaouz, E.H., Apaéstegui, J., Guyot, J.L., 2017. Speleothem records

659 decadal to multidecadal hydroclimate variations in southwestern Morocco during the last

660 millennium. *Earth Planet. Sci. Lett.*, 476, 1-10. <https://doi.org/10.1016/j.epsl.2017.07.045>

661 Andrade, C., Cruz, J. V., Viveiros, F., Coutinho, R. 2019. CO₂ flux from volcanic lakes in the

662 western group of the Azores Archipelago (Portugal). *Water*, 11(3), 599.

663 <https://doi.org/10.3390/w11030599>

664 Andrade, C., Trigo R.M., Freitas, M.C., Gallego M.C., Borges, P., Ramos, A.M., 2008.

665 Comparing historic records of storm frequency and the North Atlantic Oscillation (NAO)

666 chronology for the Azores region. *Holocene*, 18, 745-754.

667 <https://doi.org/10.1177/0959683608091794>

668 Antunes, P., Rodrigues, F. C., 2011. Azores Volcanic Lakes: factors affecting water

669 quality. *Water Quality: Currents Trends and Expected Climate Change Impacts*, 106-114.

670 Araguás-Araguás, L., Froehlich, K., & Rozanski, K., 2000. Deuterium and oxygen-18 isotope

671 composition of precipitation and atmospheric moisture. *Hydrol. Process.*, 14(8), 1341-1355.

672 [https://doi.org/10.1002/1099-1085\(20000615\)14:8<1341::AID-HYP983>3.0.CO;2-Z](https://doi.org/10.1002/1099-1085(20000615)14:8<1341::AID-HYP983>3.0.CO;2-Z)

673 Auguet, J. C., Nomokonova, N., Camarero, L., Casamayor, E. O., 2011. Seasonal changes of
674 freshwater ammonia-oxidizing archaeal assemblages and nitrogen species in oligotrophic
675 alpine lakes. *Appl. Environ. Microbiol.*, 77(6), 1937-1945.
676 <https://doi.org/10.1128/AEM.01213-10>

677 Auguet, J. C., Triado-Margarit, X., Nomokonova, N., Camarero, L., & Casamayor, E. O. (2012).
678 Vertical segregation and phylogenetic characterization of ammonia-oxidizing Archaea in a
679 deep oligotrophic lake. *ISME J.*, 6(9), 1786-1797. <https://doi.org/10.1038/ismej.2012.33>

680 Balascio, N. L., D'Andrea, W. J., Anderson, R. S., Wickler, S., 2018. Influence of vegetation
681 type on n-alkane composition and hydrogen isotope values from a high latitude ombrotrophic
682 bog. *Org. Geochem.*, 121, 48-57. <https://doi.org/10.1016/j.orggeochem.2018.03.008>

683 Baldini, L. M., McDermott, F., Foley, A. M., Baldini, J. U., 2008. Spatial variability in the
684 European winter precipitation $\delta^{18}\text{O}$ -NAO relationship: Implications for reconstructing NAO-
685 mode climate variability in the Holocene. *Geophys. Res. Lett.*, 35(4).
686 <https://doi.org/10.1029/2007GL032027>

687 Bernárdez, P., Prego, R., Francés, G., González-Álvarez, R., 2005. Opal content in the Ría de
688 Vigo and Galician continental shelf: biogenic silica in the muddy fraction as an accurate
689 paleoproductivity proxy. *Cont. Shelf Res.*, 25(10), 1249-1264.
690 <https://doi.org/10.1016/j.csr.2004.12.009>

691 Blaga, C. I., Reichart, G. J., Heiri, O., Damsté, J. S. S., 2009. Tetraether membrane lipid
692 distributions in water-column particulate matter and sediments: a study of 47 European lakes
693 along a north–south transect. *J. Paleolimnol.*, 41(3), 523-540. [https://doi.org/10.1007/s10933-](https://doi.org/10.1007/s10933-008-9242-2)
694 [008-9242-2](https://doi.org/10.1007/s10933-008-9242-2)

695 Blaga, C. I., Reichart, G. J., Vissers, E. W., Lotter, A. F., Anselmetti, F. S., Damsté, J. S. S.,
696 2011. Seasonal changes in glycerol dialkyl glycerol tetraether concentrations and fluxes in a
697 perialpine lake: Implications for the use of the TEX₈₆ and BIT proxies. *Geochim.*
698 *Cosmochim. Acta*, 75(21), 6416-6428. <https://doi.org/10.1016/j.gca.2011.08.016>

699 Blaauw, M., Christen, J. A., Vazquez, J. E., Goring, S., Clam - Classical Age-Depth
700 Modelling of Cores from Deposits. R Packag. Version 2.3.9 (2020)

701 Björck, S., Rittenour, T., Rosén, P., França, Z., Möller, P., Snowball, I., Wastegård, S., Bennike,
702 O., Kromer, B., 2006. A Holocene lacustrine record in the central North Atlantic: proxies for
703 volcanic activity, short-term NAO mode variability, and long-term precipitation
704 changes. *Quat. Sci. Rev.*, 25(1-2), 9-32. <https://doi.org/10.1016/j.quascirev.2005.08.008>

705 Borges, P. A. V., Santos, A. M. C., Elias, R. B., & Gabriel, R. (2019). The Azores Archipelago:
706 Biodiversity Erosion and Conservation Biogeography. Reference Module in Earth Systems
707 and Environmental Sciences. <https://doi.org/10.1016/b978-0-12-409548-9.11949-9>

708 Brenner, M., Whitmore, T. J., Curtis, J. H., Hodell, D. A., Schelske, C. L., 1999. Stable isotope
709 ($\delta^{13}\text{C}$ and $\delta^{15}\text{N}$) signatures of sedimented organic matter as indicators of historic lake trophic
710 state. *J. Paleolimnol.*, 22(2), 205-221. <https://doi.org/10.1007/s10933-012-9593-6>

711 Buckles, L. K., Villanueva, L., Weijers, J. W., Verschuren, D., Damsté, J. S. S., 2013. Linking
712 isoprenoidal GDGT membrane lipid distributions with gene abundances of ammonia-
713 oxidizing Thaumarchaeota and uncultured crenarchaeotal groups in the water column of a
714 tropical lake (Lake Challa, East Africa). *Environ. Microbiol.*, 15(9), 2445-2462.
715 <https://doi.org/10.1111/1462-2920.12118>

716 Bull, I. D., Lockheart, M. J., Elhmmali, M. M., Roberts, D. J., Evershed, R. P., 2002. The origin
717 of faeces by means of biomarker detection. *Environ. Int.*, 27(8), 647-654.
718 [https://doi.org/10.1016/s0160-4120\(01\)00124-6](https://doi.org/10.1016/s0160-4120(01)00124-6)

719 Calado, H., Borges, P., Phillips, M., Ng, K., Alves, F., 2011. The Azores archipelago, Portugal:
720 improved understanding of small island coastal hazards and mitigation measures. *Nat*
721 *Hazards* 58, 427–444. <https://doi.org/10.1007/s11069-010-9676-5>

722 Castilla-Beltrán, A., de Nascimento, L., Fernández-Palacios, J. M., Fonville, T., Whittaker, R. J.,
723 Edwards, M., Nogué, S., 2019. Late Holocene environmental change and the anthropization
724 of the highlands of Santo Antão Island, Cabo Verde. *Palaeogeogr., Palaeoclimatol.,*
725 *Palaeoecol.*, 524, 101-117. <https://doi.org/10.1016/j.palaeo.2019.03.033>

726 Connor, S. E., van Leeuwen, J. F., Rittenour, T. M., van der Knaap, W. O., Ammann, B., Björck,
727 S., 2012. The ecological impact of oceanic island colonization—a palaeoecological
728 perspective from the Azores. *J. Biogeogr.*, 39(6), 1007-1023. [https://doi.org/10.1111/j.1365-](https://doi.org/10.1111/j.1365-2699.2011.02671.x)
729 [2699.2011.02671.x](https://doi.org/10.1111/j.1365-2699.2011.02671.x)

730 Cordeiro, R., Luz, R., Vilaverde, J., Vasconcelos, V., Fonseca, A., Gonçalves, V., 2020.
731 Distribution of Toxic Cyanobacteria in Volcanic Lakes of the Azores Islands. *Water*, 12(12),
732 3385. <https://doi.org/10.3390/w12123385>

733 Craig, H., 1961. Isotopic variations in meteoric waters. *Science*, 133(3465), 1702-1703.
734 <https://doi.org/10.1126/science.133.3465.1702>

735 Cranwell, P. A., 1973. Chain-length distribution of *n*-alkanes from lake sediments in relation to
736 post-glacial environmental change. *Freshw. Biol.*, 3(3), 259-265.
737 <https://doi.org/10.1111/j.1365-2427.1973.tb00921.x>

738 Cropper, T. E., Hanna, E., 2014. An analysis of the climate of Macaronesia, 1865–2012. *Int. J.*
739 *Climatol.*, 34(3), 604-622. <https://doi.org/10.1002/joc.3710>

740 Crosby, A. W. (2004). *Ecological imperialism: the biological expansion of Europe, 900-1900.*
741 Cambridge University Press.

742 Cruz, J. V., Pacheco, D., Porteiro, J., Cymbron, R., Mendes, S., Malcata, A., Andrade, C., 2015.
743 Sete Cidades and Furnas lake eutrophication (São Miguel, Azores): Analysis of long-term
744 monitoring data and remediation measures. *Sci. Total Environ.*, 520, 168-186.
745 <https://doi.org/10.1016/j.scitotenv.2015.03.052>

746 Dansgaard, W., 1964. Stable isotopes in precipitation. *Tellus*, 16(4), 436-468.
747 <https://doi.org/10.1111/j.2153-3490.1964.tb00181.x>

748 de Nascimento, L., Willis, K. J., Fernández-Palacios, J. M., Criado, C., Whittaker, R. J., 2009.
749 The long-term ecology of the lost forests of La Laguna, Tenerife (Canary Islands). *J.*
750 *Biogeogr.*, 36(3), 499-514. <https://doi.org/10.1111/j.1365-2699.2008.02012.x>

751 Dias, E., Mendes, C., Melo, C., Pereira, D., Elias, R., 2005. Azores Central Islands vegetation
752 and flora field guide. *Quercetea*, 7, 123-173.

753 Dickinson, C. H., & Underhay, V. H. S., 1977. Growth of fungi in cattle dung. *Trans. Brit.*
754 *Mycol. Soc.*, 69(3), 473-477. [https://doi.org/10.1016/S0007-1536\(77\)80086-7](https://doi.org/10.1016/S0007-1536(77)80086-7)

755 Diefendorf, A. F., Freeman, K. H., Wing, S. L., Graham, H. V., 2011. Production of n-alkyl
756 lipids in living plants and implications for the geologic past. *Geochim. Cosmochim. Acta*,
757 75(23), 7472-7485. <https://doi.org/10.1016/j.gca.2011.09.028>

758 Douglas, M. S., Smol, J. P., Savelle, J. M., Blais, J. M., 2004. Prehistoric Inuit whalers affected
759 Arctic freshwater ecosystems. *Proc. Nat. Acad. Sci.*, 101(6), 1613-1617.
760 <https://doi.org/10.1073/pnas.0307570100>

761 Ekdahl, E. J., Teranes, J. L., Guilderson, T. P., Turton, C. L., McAndrews, J. H., Wittkop, C. A.,
762 Stoermer, E. F., 2004. Prehistorical record of cultural eutrophication from Crawford Lake,
763 Canada. *Geology*, 32(9), 745-748. <https://doi.org/10.1130/G20496.1>

764 Esper, J., Frank, D., Büntgen, U., Verstege, A., Luterbacher, J., Xoplaki, E. 2007. Long-term
765 drought severity variations in Morocco. *Geophys. Res. Lett.*, 34(17).
766 <https://doi.org/10.1029/2007GL030844>

767 Frias, R., 2000. EUROSION Case Study.

768 Gaskell, S. J., Eglinton, G., 1975. Rapid hydrogenation of sterols in a contemporary lacustrine
769 sediment. *Nature*, 254(5497), 209-211. <https://doi.org/10.1038/254209b0>

770 Gill, J. L., McLauchlan, K. K., Skibbe, A. M., Goring, S., Zirbel, C. R., Williams, J. W., 2013.
771 Linking abundances of the dung fungus *Sporormiella* to the density of bison: implications for
772 assessing grazing by megaherbivores in palaeorecords. *J. Ecol.*, 101(5), 1125-1136.
773 <https://doi.org/10.1111/1365-2745.12130>

774 Gimeno L., Nieto R., Trigo R.M., Vicente-Serrano S.M, Lopes-Moreno J.I., 2010. Where does
775 the Iberian Peninsula moisture come from? An answer based on a Lagrangian approach. *J.*
776 *Hydrometeorol.*, 11, 421-436. <https://doi.org/10.1175/2009JHM1182.1>

777 *Global Historical Climatology Network (GHCN)*. NOAA, <https://www.ncdc.noaa.gov/>

778 Gordo, C., Zêzere, J. L., Marques, R., 2019. Landslide susceptibility assessment at the basin
779 scale for rainfall-and earthquake-triggered shallow slides. *Geosciences*, 9(6), 268.
780 <https://doi.org/10.3390/geosciences9060268>

781 Guillemot, T., Bichet, V., Gauthier, E., Zocatelli, R., Massa, C., Richard, H. 2017.
782 Environmental responses of past and recent agropastoral activities on south Greenlandic

783 ecosystems through molecular biomarkers. *Holocene*, 27(6), 783-795.
784 <https://doi.org/10.1177/0959683616675811>

785 Hannon, G. E., Bradshaw, R. H., Bradshaw, E. G., Snowball, I., Wastegård, S., 2005. Climate
786 change and human settlement as drivers of late-Holocene vegetational change in the Faroe
787 Islands. *Holocene*, 15(5), 639-647. <https://doi.org/10.1191/0959683605hl840rp>

788 Hernández, A., Kutiel, H., Trigo, R. M., Valente, M. A., Sigró, J., Cropper, T., Santo, F. E.,
789 2016. New Azores Archipelago daily precipitation dataset and its links with large-scale
790 modes of climate variability. *Int. J. Climatol.*, 36(14), 4439-4454.
791 <https://doi.org/10.1002/joc.4642>

792 Hernández, A., Sáez, A., Bao, R., Raposeiro, P.M., Trigo, R.M., Doolittle, S., Masqué, P., Rull,
793 V., Gonçalves, V., Vázquez-Loureiro, D., Rubio-Inglés, M.J., 2017. The influences of the
794 AMO and NAO on the sedimentary infill in an Azores Archipelago lake since ca. 1350
795 CE. *Glob. Planet. Change*, 154, 61-74. <https://doi.org/10.1016/j.gloplacha.2017.05.007>

796 Hillbrand, M., van Geel, B., Hasenfratz, A., Hadorn, P., Haas, J. N., 2014. Non-pollen
797 palynomorphs show human-and livestock-induced eutrophication of Lake Nussbaumersee
798 (Thurgau, Switzerland) since Neolithic times (3840 BC). *Holocene*, 24(5), 559-568.
799 <https://doi.org/10.1177/0959683614522307>

800 Hodell, D. A., Schelske, C. L., 1998. Production, sedimentation, and isotopic composition of
801 organic matter in Lake Ontario. *Limnol. Oceanogr.*, 43(2), 200-214.
802 <https://doi.org/10.4319/lo.1998.43.2.0200>

803 Hoegh-Guldberg, O., D. Jacob, M. Taylor, M. Bindi, S. Brown, I. Camilloni, A. Diedhiou, R.
804 Djalante, K.L. Ebi, F. Engelbrecht, J. Guiot, Y. Hijioaka, S. Mehrotra, A. Payne, S.I.
805 Seneviratne, A. Thomas, R. Warren, G. Zhou, 2018: Impacts of 1.5°C Global Warming on

806 Natural and Human Systems. In: *Global Warming of 1.5°C. An IPCC Special Report on the*
807 *impacts of global warming of 1.5°C above pre-industrial levels and related global*
808 *greenhouse gas emission pathways, in the context of strengthening the global response to the*
809 *threat of climate change, sustainable development, and efforts to eradicate poverty* [Masson-
810 Delmotte, V., P. Zhai, H.-O. Pörtner, D. Roberts, J. Skea, P.R. Shukla, A. Pirani, W.
811 Moufouma-Okia, C. Pan, R. Pidcock, S. Connors, J.B.R. Matthews, Y. Chen, X. Zhou, M.I.
812 Gomis, E. Lonnoy, T. Maycock, M. Tignor, and T. Waterfield (eds.)].

813 Hollander, D. J., Smith, M. A., 2001. Microbially mediated carbon cycling as a control on the
814 $\delta^{13}\text{C}$ of sedimentary carbon in eutrophic Lake Mendota (USA): new models for interpreting
815 isotopic excursions in the sedimentary record. *Geochim. Cosmochim. Acta*, 65(23), 4321-
816 4337. [https://doi.org/10.1016/S0016-7037\(00\)00506-8](https://doi.org/10.1016/S0016-7037(00)00506-8)

817 Hopmans, E. C., Schouten, S., Damsté, J. S. S., 2016. The effect of improved chromatography on
818 GDGT-based palaeoproxies. *Org. Geochem.*, 93, 1-6.
819 <https://doi.org/10.1016/j.orggeochem.2015.12.006>

820 Huang, W. Y., Meinschein, W. G., 1976. Sterols as source indicators of organic materials in
821 sediments. *Geochim. Cosmochim. Acta*, 40(3), 323-330. [https://doi.org/10.1016/0016-](https://doi.org/10.1016/0016-7037(76)90210-6)
822 [7037\(76\)90210-6](https://doi.org/10.1016/0016-7037(76)90210-6)

823 Huang, W. Y., Meinschein, W. G., 1979. Sterols as ecological indicators. *Geochim. Cosmochim.*
824 *Acta*, 43(5), 739-745. [https://doi.org/10.1016/0016-7037\(79\)90257-6](https://doi.org/10.1016/0016-7037(79)90257-6)

825 Huguet, C., Hopmans, E. C., Febo-Ayala, W., Thompson, D. H., Damsté, J. S. S., Schouten, S.,
826 2006. An improved method to determine the absolute abundance of glycerol dibiphytanyl
827 glycerol tetraether lipids. *Org. Geochem.*, 37(9), 1036-1041.
828 <https://doi.org/10.1016/j.orggeochem.2006.05.008>

829 Hurrell, J. W., 1995. Decadal trends in the North Atlantic Oscillation: regional temperatures and
830 precipitation. *Science*, 269(5224), 676-679. <https://doi.org/10.1126/science.269.5224.676>
831 *IAEA/WMO: Global Network of Isotopes in Precipitation. The GNIP Database*,
832 2006, <http://www.iaea.org/water>.

833 Kalff, J., 2002. *Limnology: inland water ecosystems*. Upper Saddle River, NJ: Prentice-Hall Inc.

834 Kumar, D. M., Woltering, M., Hopmans, E. C., Damsté, J. S. S., Schouten, S., Werne, J. P.,
835 2019. The vertical distribution of Thaumarchaeota in the water column of Lake Malawi
836 inferred from core and intact polar tetraether lipids. *Org. Geochem.*, 132, 37-49.
837 <https://doi.org/10.1016/j.orggeochem.2019.03.004>

838 Lages, G., 2000. Situação das Flores e do Corvo nos séculos XVI e XVII. *Arquipélago - História*
839 2, 29–88.

840 Lawson, I.T., Church, M.J., McGovern, T.H., Arge, S.V., Woollet, J., Edwards, K.J., Gathorne-
841 Hardy, F.J., Dugmore, A.J., Cook, G., Mairs, K.A., Thomson, A.M., 2005. Historical ecology
842 on Sandoy, Faroe Islands: palaeoenvironmental and archaeological perspectives. *Hum.*
843 *Ecol.*, 33(5), 651-684. <https://doi.org/10.1007/s10745-005-7681-1>

844 Lawson, I. T., Gathorne-Hardy, F. J., Church, M. J., Newton, A. J., Edwards, K. J., Dugmore, A.
845 J., Einarsson, A., 2007. Environmental impacts of the Norse settlement: palaeoenvironmental
846 data from Mývatnssveit, northern Iceland. *Boreas*, 36(1), 1-19.
847 <https://doi.org/10.1111/j.1502-3885.2007.tb01176.x>

848 Leeming, R., Ball, A., Ashbolt, N., Nichols, P., 1996. Using faecal sterols from humans and
849 animals to distinguish faecal pollution in receiving waters. *Water Res.*, 30(12), 2893-2900.
850 [https://doi.org/10.1016/S0043-1354\(96\)00011-5](https://doi.org/10.1016/S0043-1354(96)00011-5)

851 Lloyd, C. E., Michaelides, K., Chadwick, D. R., Dungait, J. A., Evershed, R. P., 2012. Tracing
852 the flow-driven vertical transport of livestock-derived organic matter through soil using
853 biomarkers. *Org. Geochem.*, 43, 56-66. <https://doi.org/10.1016/j.orggeochem.2011.11.001>

854 Maffei, M., 1996. Chemotaxonomic significance of leaf wax alkanes in the
855 Gramineae. *Biochem. Syst. Ecol.*, 24(1), 53-64. [https://doi.org/10.1016/0305-](https://doi.org/10.1016/0305-1978(95)00102-6)
856 [1978\(95\)00102-6](https://doi.org/10.1016/0305-1978(95)00102-6)

857 Marques R., Zezere J.L., Trigo R.M., Gaspar J.L., Trigo I.F., 2008. Rainfall patterns and critical
858 values associated with landslides in Povoação County (São Miguel Island, Azores):
859 relationships with the North Atlantic Oscillation. *Hydrol. Process.*, 22, 478-494, DOI:
860 [10.1002/hyp.6879](https://doi.org/10.1002/hyp.6879).

861 Marsden, M. W., 1989. Lake restoration by reducing external phosphorus loading: the influence
862 of sediment phosphorus release. *Freshw. Biol.*, 21(2), 139-162.
863 <https://doi.org/10.1111/j.1365-2427.1989.tb01355.x>

864 Massa, C., Bichet, V., Gauthier, É., Perren, B.B., Mathieu, O., Petit, C., Monna, F., Giraudeau,
865 J., Losno, R., Richard, H., 2012. A 2500 year record of natural and anthropogenic soil
866 erosion in South Greenland. *Quat. Sci. Rev.*, 32, 119-130.
867 <https://doi.org/10.1016/j.quascirev.2011.11.014>

868 Meneses, A. de F. de, 2009. Os Açores e os Impérios - séculos XV a XX. *Arquipélago - História*
869 *XIII*, 205–218.

870 Meyers, P. A., 2003. Applications of organic geochemistry to paleolimnological reconstructions:
871 a summary of examples from the Laurentian Great Lakes. *Org. Geochem.*, 34(2), 261-289.
872 [https://doi.org/10.1016/S0146-6380\(02\)00168-7](https://doi.org/10.1016/S0146-6380(02)00168-7)

873 Mortlock, R. A., Froelich, P. N., 1989. A simple method for the rapid determination of biogenic
874 opal in pelagic marine sediments. *Deep Sea Res. Part A. Oceanogr. Res. Pap.*, 36(9), 1415-
875 1426. [https://doi.org/10.1016/0198-0149\(89\)90092-7](https://doi.org/10.1016/0198-0149(89)90092-7)

876 Muggeo, V.M., 2008. segmented: an R Package to Fit Regression Models with Broken-Line
877 Relationships. *R News*, 8(1), 20–25. <https://cran.r-project.org/doc/Rnews/>.

878 Naeher, S., Peterse, F., Smittenberg, R. H., Niemann, H., Zigah, P. K., Schubert, C. J., 2014.
879 Sources of glycerol dialkyl glycerol tetraethers (GDGTs) in catchment soils, water column
880 and sediments of Lake Rotsee (Switzerland)—Implications for the application of GDGT-based
881 proxies for lakes. *Org. Geochem.*, 66, 164-173.
882 <https://doi.org/10.1016/j.orggeochem.2013.10.017>

883 Nishimura, M., Koyama, T., 1977. The occurrence of stanols in various living organisms and the
884 behavior of sterols in contemporary sediments. *Geochim. Cosmochim. Acta*, 41(3), 379-385.
885 [https://doi.org/10.1016/0016-7037\(77\)90265-4](https://doi.org/10.1016/0016-7037(77)90265-4)

886 Nishimura, M., 1977. Origin of stanols in young lacustrine sediments. *Nature*, 270(5639), 711-
887 712. <https://doi.org/10.1038/270711a0>

888 Pancost, R.D., van Geel, B., Baas, M., Sinninghe Damsté, J.S., 2000. $\delta^{13}\text{C}$ values and
889 radiocarbon dates of microbial biomarkers as tracers for carbon recycling in peat deposits.
890 *Geology*, 28, 663–666. [https://doi.org/10.1130/0091-
891 7613\(2000\)28<663:CVARDO>2.0.CO;2](https://doi.org/10.1130/0091-7613(2000)28<663:CVARDO>2.0.CO;2)

892 Pancost, R.D., Hopmans, E.C., Sinninghe Damsté, J.S., 2001. Archaeal lipids in Mediterranean
893 cold seeps: molecular proxies for anaerobic methane oxidation. *Geochim. Cosmochim. Acta*,
894 65, 1611–1627. [https://doi.org/10.1016/S0016-7037\(00\)00562-7](https://doi.org/10.1016/S0016-7037(00)00562-7)

895 Pearson, A., Huang, Z., Ingalls, A.E., Romanek, C.S., Wiegel, J., Freeman, K.H., Smittenberg,
896 R.H., Zhang, C.L., 2004. Nonmarine crenarchaeol in Nevada hot springs. *Appl. Environ.*
897 *Microbiol.*, 70(9), 5229-5237. <https://doi.org/10.1128/AEM.70.9.5229-5237.2004>

898 Perrotti, A.G., van Asperen, E., 2019. Dung fungi as a proxy for megaherbivores: opportunities
899 and limitations for archaeological applications. *Veget. Hist. Archaeobot.* 28, 93–104.
900 <https://doi.org/10.1007/s00334-018-0686-7>

901 Pitcher, A., Rychlik, N., Hopmans, E.C., Spieck, E., Rijpstra, W.I.C., Ossebaar, J., Schouten, S.,
902 Wagner, M., Sinninghe Damsté, J.S.S., 2010. Crenarchaeol dominates the membrane lipids
903 of *Candidatus Nitrososphaera gargensis*, a thermophilic Group I. 1b Archaeon. *ISME*
904 *J.*, 4(4), 542-552. <https://doi.org/10.1038/ismej.2009.138>

905 Pitcher, A., Hopmans, E.C., Mosier, A.C., Park, S.J., Rhee, S.K., Francis, C.A., Schouten, S.,
906 Sinninghe Damsté, J.S., 2011. Core and intact polar glycerol dibiphytanyl glycerol tetraether
907 lipids of ammonia-oxidizing archaea enriched from marine and estuarine sediments. *Appl.*
908 *Environ. Microbiol.*, 77(10), 3468-3477. <https://doi.org/10.1128/AEM.02758-10>

909 Pouliot, J., Galand, P. E., Lovejoy, C., Vincent, W. F., 2009. Vertical structure of archaeal
910 communities and the distribution of ammonia monooxygenase A gene variants in two
911 meromictic High Arctic lakes. *Environ. Microbiol.*, 11(3), 687-699.
912 <https://doi.org/10.1111/j.1462-2920.2008.01846.x>

913 Raposeiro, P.M., Hernández, A., Pla-Rabes, S., Bao, R. Sáez, A., Benavente, M. Richter, N., de
914 Groff, W., de Boer, E.J., Ritter, C. Amaral-Zettler, L.A., Giralt, S. 2021a. Multi-proxy
915 analysis of sediment cores from Lake Funda (Azores Archipelago, Portugal). *PANGAEA*,
916 <https://doi.org/10.1594/PANGAEA.933712>

917 Raposeiro, P.M., Hernández, A., Pla-Rabes, S., Gonçalves, V., Bao, R., Sáez, A., Shanahan, T.,
918 Benavente, M., de Boer, E., Richter, N., Gordon, V., Marques, H., Sousa, P.M., Souto, M.,
919 Matias, M.G., Aguiar, N., Pereira, C., Ritter, C., Rubio, M.J., Salcedo, M., Vázquez-
920 Loureiro, D., Margalef, O., Amaral-Zettler, L.A., Costa, A.C., Huang, Y., van Leeuwen,
921 J.F.N., Masqué, P., Prego, R., Ruiz-Fernández, A.C., Sánchez-Cabeza, J., Trigo, R., Giralt,
922 S., 2021b. Climate change facilitated the early colonization of the Azores Archipelago during
923 Medieval times. *Proc. Natl. Acad. Sci.*, 118(41), e2108236118.
924 <https://doi.org/10.1073/pnas.2108236118>

925 Raposeiro, P.M., Rubio, M.J., González, A., Hernández, A., Sánchez-López, G., Vázquez-
926 Loureiro, D., Rull, V., Bao, R., Costa, A.C., Gonçalves, V., Sáez, A., 2017. Impact of the
927 historical introduction of exotic fishes on the chironomid community of Lake Azul (Azores
928 Islands). *Palaeogeogr., Palaeoclimatol., Palaeoecol.*, 466, 77-88.
929 <https://doi.org/10.1016/j.palaeo.2016.11.015>

930 Reimer, P.J., Bard, E., Bayliss, A., Beck, J.W., Blackwell, P.G., Ramsey, C.B., Buck, C.E.,
931 Cheng, H., Edwards, R.L., Friedrich, M., Grootes, P.M., Guilderson, T.P., Haflidason, H.,
932 Hajdas, I., Hatté, C., Heaton, T.J., Hoffmann, D.L., Hogg, A.G., Hughen, K.A., Kaiser, K.F.,
933 Kromer, B., Manning, S.W., Niu, M., Reimer, R.W., Richards, D.A., Scott, E.M., Southon,
934 J.R., Staff, R.A., Turney, C.S.M., van der Plicht, J., 2013. IntCal13 and Marine13
935 radiocarbon age calibration curves 0–50,000 years cal BP. *Radiocarbon*, 55, 1869–1887.
936 https://doi.org/10.2458/azu_js_rc.55.16947

937 Richter, N., Russell, J.M., Garfinkel, J., Huang, Y., 2021. Impacts of Norse settlement on
938 terrestrial and aquatic ecosystems in Southwest Iceland. *J. Paleolimnol.*, 65(2), 255-269.
939 <https://doi.org/10.1007/s10933-020-00169-3>

940 Richter, N., Russell, J. M., Amaral-Zettler, L. A., DeGroot, W., Raposeiro, P.M., Gonçalves, V.,
941 Pla-Rabes, S., Hernández, A., Benavente, M., Ritter, C., Bao, R., Prego, R., Giralt, S., 2022.
942 Organic geochemical analysis of sediment cores from Lake Funda (Azores Archipelago,
943 Portugal). PANGAEA, <https://doi.org/10.1594/PANGAEA.941316>

944 Ritter, C., Gonçalves, V., Pla-Rabes, S., de Boer, E.J., Bao, R., Sáez, A., Hernández, A., Sixto,
945 M., Richter, N., Benavente, M., Prego, R., Giralt, S., Raposeiro, P.M., 2022. The vanishing
946 and the establishment of a new ecosystem on an oceanic island – Anthropogenic impacts
947 with no return ticket. *Sci. Total Environ.* 154828.
948 <https://doi.org/10.1016/j.scitotenv.2022.154828>

949 Rubio de Inglés, M. J., 2016. Late Holocene Climate Variability in the North Atlantic based on
950 biomarker reconstruction: The lake Azul (São Miguel, Azores Archipelago) case.

951 Rull, V., Lara, A., Rubio-Inglés, M.J., Giralt, S., Gonçalves, V., Raposeiro, P., Hernández, A.,
952 Sánchez-López, G., Vázquez-Loureiro, D., Bao, R., Masqué, P., 2017. Vegetation and
953 landscape dynamics under natural and anthropogenic forcing on the Azores Islands: A 700-
954 year pollen record from the São Miguel Island. *Quat. Sci. Rev.*, 159, 155-168.
955 <https://doi.org/10.1016/j.quascirev.2017.01.021>

956 Sachse, D., Billault, I., Bowen, G.J., Chikaraishi, Y., Dawson, T.E., Feakins, S.J., Freeman,
957 K.H., Magill, C.R., McInerney, F.A., Van Der Meer, M.T., Polissar, P., 2012. Molecular
958 paleohydrology: interpreting the hydrogen-isotopic composition of lipid biomarkers from
959 photosynthesizing organisms. *Annu. Rev. Earth Planet. Sci.*, 40, 221-249.
960 <https://doi.org/10.1146/annurev-earth-042711-105535>

961 Sánchez-López, G., Hernández, A., Pla-Rabès, S., Trigo, R.M., Toro, M., Granados, I., Sáez, A.,
962 Masqué, P., Pueyo, J.J., Rubio-Inglés, M.J., Giralt, S., 2016. Climate reconstruction for the

963 last two millennia in central Iberia: The role of East Atlantic (EA), North Atlantic Oscillation
964 (NAO) and their interplay over the Iberian Peninsula. *Quat. Sci. Rev.*, 149, 135-150.
965 <https://doi.org/10.1016/j.quascirev.2016.07.021>

966 Santos, F. D., Valente, M. A., Miranda, P. M. A., Aguiar, A., Azevedo, E. B., Tomé, A. R.,
967 Coelho, F., 2004. Climate change scenarios in the Azores and Madeira Islands. *World*
968 *Resour. Rev.*, 16(4), 473-491.

969 Schäfer, H., 2003. Chorology and diversity of the Azorean flora. *Willdenowia*, 33, 481-482.

970 Scheffer, M., 1998. *Ecology of shallow lakes* (Vol. 1). London: Chapman & Hall.

971 Scheffer, M., Carpenter, S., Foley, J. A., Folke, C., Walker, B., 2001. Catastrophic shifts in
972 ecosystems. *Nature*, 413(6856), 591-596. <https://doi.org/10.1038/35098000>

973 Schindler, D. W., 2006. Recent advances in the understanding and management of
974 eutrophication. *Limnol. Oceanogr.*, 51, 356-363.
975 https://doi.org/10.4319/lo.2006.51.1_part_2.0356

976 Schouten, S., Hopmans, E.C., Baas, M., Boumann, H., Standfest, S., Könneke, M., Stahl, D.A.,
977 Sinninghe Damsté, J.S., 2008. Intact membrane lipids of “*Candidatus Nitrosopumilus*
978 *maritimus*,” a cultivated representative of the cosmopolitan mesophilic group I
979 Crenarchaeota. *Appl. Environ. Microbiol.*, 74(8), 2433-2440.
980 <https://doi.org/10.1128/AEM.01709-07>

981 Schouten, S., Hopmans, E. C., Damsté, J. S. S., 2013. The organic geochemistry of glycerol
982 dialkyl glycerol tetraether lipids: a review. *Org. Geochem.*, 54, 19-61.
983 <https://doi.org/10.1016/j.orggeochem.2012.09.006>

984 Schwark, L., Zink, K., Lechterbeck, J., 2002. Reconstruction of postglacial to early Holocene
985 vegetation history in terrestrial Central Europe via cuticular lipid biomarkers and pollen

986 records from lake sediments. *Geology*, 30(5), 463-466. <https://doi.org/10.1130/0091->
987 7613(2002)030<0463:ROPTEH>2.0.CO;2

988 Sinninghe Damsté, J. S., Schouten, S., Hopmans, E. C., Van Duin, A. C., Geenevasen, J. A.,
989 2002. Crenarchaeol. *J. Lipid Res.*, 43(10), 1641-1651. <https://doi.org/10.1194/jlr.M200148->
990 JLR200

991 Sinninghe Damsté, J. S., Ossebaar, J., Abbas, B., Schouten, S., Verschuren, D., 2009. Fluxes and
992 distribution of tetraether lipids in an equatorial African lake: constraints on the application of
993 the TEX₈₆ palaeothermometer and BIT index in lacustrine settings. *Geochim. Cosmochim.*
994 *Acta*, 73(14), 4232-4249. <https://doi.org/10.1016/j.gca.2009.04.022>

995 Sinninghe Damsté, J.S., Rijpstra, W.I.C., Hopmans, E.C., Jung, M.Y., Kim, J.G., Rhee, S.K.,
996 Stieglmeier, M., Schleper, C., 2012. Intact polar and core glycerol dibiphytanyl glycerol
997 tetraether lipids of group I. 1a and I. 1b Thaumarchaeota in soil. *App. Environ.*
998 *Microbiol.*, 78(19), 6866-6874. <https://doi.org/10.1128/AEM.01681-12>

999 Skov, T., Buchaca, T., Amsinck, S.L., Landkildehus, F., Odgaard, B.V., Azevedo, J., Gonçalves,
1000 V., Raposeiro, P.M., Andersen, T.J., Jeppesen, E., 2010. Using invertebrate remains and
1001 pigments in the sediment to infer changes in trophic structure after fish introduction in Lake
1002 Fogo: a crater lake in the Azores. *Hydrobiologia*, 654(1), 13-25.
1003 <https://doi.org/10.1007/s10750-010-0325-5>

1004 Smith, S. H., 2010. The mid-Atlantic islands: A theatre of early modern ecocide?. *Int. Rev. Soc.*
1005 *Hist.*, 55(S18), 51-77.

1006 Tipple, B. J., Berke, M. A., Doman, C. E., Khachatryan, S., Ehleringer, J. R. 2013. Leaf-wax n-
1007 alkanes record the plant–water environment at leaf flush. *Proc. Nat. Acad. Sci.*, 110(7), 2659-
1008 2664. <https://doi.org/10.1073/pnas.1213875110>

1009 van Bree, L.G.J., Peterse, F., Van der Meer, M.T.J., Middelburg, J.J., Negash, A.M.D., De Crop,
1010 W., Cocquyt, C., Wieringa, J.J., Verschuren, D., Damsté, J.S., 2018. Seasonal variability in
1011 the abundance and stable carbon-isotopic composition of lipid biomarkers in suspended
1012 particulate matter from a stratified equatorial lake (Lake Chala, Kenya/Tanzania):
1013 Implications for the sedimentary record. *Quat. Sci. Rev.*, 192, 208-224.
1014 <https://doi.org/10.1016/j.quascirev.2018.05.023>

1015 Vázquez-Loureiro, D., Gonçalves, V., Sáez, A., Hernández, A., Raposeiro, P.M., Giralt, S.,
1016 Rubio-Inglés, M.J., Rull, V. and Bao, R., 2019. Diatom-inferred ecological responses of an
1017 oceanic lake system to volcanism and anthropogenic perturbations since 1290 CE.
1018 *Palaeogeogr., Palaeoclimatol., Palaeoecol.*, 534, p.109285.
1019 <https://doi.org/10.1016/j.palaeo.2019.109285>

1020 Volkman, J. K., 1986. A review of sterol markers for marine and terrigenous organic matter.
1021 *Org. Geochem.*, 9(2), 83-99. [https://doi.org/10.1016/0146-6380\(86\)90089-6](https://doi.org/10.1016/0146-6380(86)90089-6)

1022 Wakeham, S. G., Lewis, C. M., Hopmans, E. C., Schouten, S., Sinninghe Damsté, J. S., 2003.
1023 Archaea mediate anaerobic oxidation of methane in deep euxinic waters of the Black
1024 Sea. *Geochim. Cosmochim. Acta*, 67(7), 1359-1374. [https://doi.org/10.1016/S0016-](https://doi.org/10.1016/S0016-7037(02)01220-6)
1025 [7037\(02\)01220-6](https://doi.org/10.1016/S0016-7037(02)01220-6)

1026 Walker, R. W., Wun, C. K., Litsky, W., & Dutka, B. J., 1982. Coprostanol as an indicator of
1027 fecal pollution. *Crit. Rev. Environ. Sci. Technol.*, 12(2), 91-112.
1028 <https://doi.org/10.1080/10643388209381695>

1029 Wassenburg, J.A., Immenhauser, A., Richter, D.K., Niedermayr, A., Riechelmann, S., Fietzke,
1030 J., Scholz, D., Jochum, K.P., Fohlmeister, J., Schröder-Ritzrau, A., Sabaoui, A., 2013.
1031 Moroccan speleothem and tree ring records suggest a variable positive state of the North

- 1032 Atlantic Oscillation during the Medieval Warm Period. *Earth Planet. Sci. Lett.*, 375, 291-302.
1033 <https://doi.org/10.1016/j.epsl.2013.05.048>
- 1034 Wood, J. R., Wilmshurst, J. M., 2012. Wetland soil moisture complicates the use of *Sporormiella*
1035 to trace past herbivore populations. *J. Quat. Sci.*, 27(3), 254-259.
1036 <https://doi.org/10.1002/jqs.1539>
- 1037 Woolway, R.I., Merchant, C.J., 2019. Worldwide alteration of lake mixing regimes in response
1038 to climate change. *Nat. Geosci.* 12, 271–276. <https://doi.org/10.1038/s41561-019-0322-x>
- 1039 Zocatelli, R., Lavrieux, M., Guillemot, T., Chassiot, L., Le Milbeau, C., Jacob, J. 2017. Fecal
1040 biomarker imprints as indicators of past human land uses: Source distinction and preservation
1041 potential in archaeological and natural archives. *J. Archaeol. Sci.*, 81, 79-89.
1042 <https://doi.org/10.1016/j.jas.2017.03.010>